NACA RM E9I16

NACA

RESEARCH MEMORANDUM

ALTITUDE-WIND-TUNNEL INVESTIGATION OF TAIL-PIPE BURNER WITH CONVERGING CONICAL BURNER SECTION ON J35-A-5 TURBOJET ENGINE

By H. Carl Thorman and Carl E. Campbell

Lewis Flight Propulsion Laboratory
Cleveland, Ohio

NATIONAL ADVISORY COMMITTEE
FOR AERONAUTICS
WASHINGTON

February 10, 1950
Declassified January 20, 1958

NATIONAL ADVISORY COMMITTEE FOR AERONAUTICS

RESEARCH MEMORANDUM

ALTITUDE-WIND-TUNNEL INVESTIGATION OF TAIL-PIPE BURNER WITH CONVERGING CONICAL BURNER SECTION ON J35-A-5 TURBOJET ENGINE

By H. Carl Thorman and Carl E. Campbell

SUMMARY

An investigation of turbojet-engine thrust augmentation by means of tail-pipe burning has been conducted in the NACA Lewis altitude wind tunnel. Results presented in this report were obtained with a tail-pipe burner designed for fuselage installation in a specific airplane. Characteristic features of this tail-pipe burner were a converging conical burner section preceded by a conical diffuser section. Three different fuel patterns and three flame holders were investigated to determine the effect of fuel distribution and flame-holder design on the tail-pipe-burner performance and operational characteristics over a range of simulated flight conditions. A conical fixed-area exhaust nozzle was used throughout the investigation.

The most efficient burner performance and the widest range of operable fuel-air ratios were obtained with configurations in which fuel injectors that gave a homogeneous distribution of the tail-pipe fuel-air mixture were used with annular-V-gutter type flame holders blocking about 30 percent of the burner cross-sectional area. The tail-pipe combustion efficiency was more severely reduced by decreasing turbine-outlet pressure below approximately 1000 pounds per square foot than at higher pressures. An increase in flight Mach number from 0.27 to 1.06 at an altitude of 25,000 feet and a turbine-outlet temperature of 1650° R increased the ratio of augmented to normal thrust from 1.43 to 1.64, with an attendant increase in exhaust-gas temperature from 3030° to 3290° R and an increase in combustion efficiency from 0.74 to 0.89. At the same conditions, the specific fuel consumption increased from 2.37 at a flight Mach number of 0.27 to 2.43 at a flight Mach number of 0.65 and then decreased to 2.32 at a flight Mach number of 1.06. At a flight Mach number of 0.27, the operable range of tail-pipe fuel-air ratios narrowed as the altitude was increased above 35,000 feet. The use of an internal cooling liner extending throughout the length of the burner section provided adequate shell cooling at all flight conditions investigated.

INTRODUCTION

In an extensive research program on thrust augmentation being conducted at the NACA Lewis laboratory, investigations (references 1 to 4) have shown that utilization of the tail-pipe-burning cycle is a practical means of increasing the thrust of turbojet engines. As part of this research program, an investigation of the effect of tail-pipe-burner design variables on burner performance and operation over a wide range of simulated flight conditions was conducted in the Lewis altitude wind tunnel. One phase of this investigation is summarized in reference 5 and another phase is presented in this report.

In order to obtain information that could be applied in the design of tail-pipe burners, a study was made to detemine the effect of flame-holder design, method of fuel injection, and burner dimensions on the following burner requirements:

1. Maximum thrust with high combustion efficiency

2. Stable burner operation over a wide range of fuel-air ratios and flight conditions

3. Adequate tail-pipe cooling

4. Dependable starting

5. Minimum loss in thrust with burner inoperative

The investigations reported in references 1 to 4 were largely exploratory and primary consideration was given to burner requirements 1 and 2. The results of these exploratory investigations provided the necessary background for investigations in which all the aforementioned burner requirements are considered.

The performance and operational characteristics of a tail-pipe burner having a converging conical burner section of $29\frac{1}{4}$-inch maximum diameter on a J35-A-5 turbojet engine were determined and are reported herein. The geometry of the tail-pipe burner was dictated by the design requirements for fuselage installation in a specific airplane. Three fuel systems, three flame holders, a cooling liner, and a tail-pipe ignition system were investigated in this burner with a fixed-area exhaust nozzle. With each configuration, data were obtained over a range of simulated flight conditions and tail-pipe fuel-air ratios.

Comparative data are presented to show the effect of fuel distribution and the type and the size of flame holder on tail-pipe burner efficiency and exhaust-gas temperature. Data are presented to show the performance variation with altitude and flight Mach number for the configurations investigated that had the highest combustion efficiency. The over-all performance of these configurations is compared with that of a similar configuration of the 29-inch-diameter cylindrical tail-pipe burner reported in reference 5. The altitude blow-out characteristics, tail-pipe shell cooling, and tail-pipe fuel ignition are also discussed.

APPARATUS

Engine

The J35-A-5 engine used in this investigation has a sea-level static thrust of 4000 pounds at a rated engine speed of 7700 rpm and a turbine-outlet temperature of 1250° F (1710° R). At this operating condition, the air flow is approximately 75 pounds per second and the fuel consumption is 4400 pounds per hour. The over-all length of the engine with the standard engine tail pipe is about 15 feet and the maximum diameter is about 38 inches. The main components of the engine are an 11-stage axial-flow compressor, eight cylindrical direct-flow-type combustion chambers, a single-stage turbine, a tail pipe, and a fixed-area exhaust nozzle. The rated operating condition of the standard engine was obtained with a $16\frac{1}{8}$-inch-diameter exhaust nozzle.

Fuel conforming to specification AN-F-32 with a lower heating value of 18,550 Btu per pound and a hydrogen-carbon ratio of 0.155 was used in the engine. Fuel conforming to specification AN-F-48b, grade 80, unleaded gasoline with a lower heating value of 19,000 Btu per pound and a hydrogen-carbon ratio of 0.186 was used in the tail-pipe burner.

Installation

For this investigation, the standard-engine tail pipe was replaced by a tail-pipe-burner assembly attached to the downstream flange of the turbine casing. The engine and the tail-pipe burner were mounted on a wing section that spanned the 20-foot-diameter test section of the altitude wind tunnel (fig. 1). In order to provide accessibility for instrumentation and modification, no cowling was installed.

Engine-inlet air pressures corresponding to altitude flight conditions were simulated by introducing dry refrigerated air from the tunnel make-up air system through a duct to the engine inlet. Air was throttled from approximately sea-level pressure to the desired pressure at the engine inlet while the static pressure in the tunnel test section was maintained to correspond to the desired altitude. A slip joint with a labyrinth seal was used in the duct, thereby making possible thrust and installation-drag measurements with the tunnel scales.

Tail-Pipe-Burner Assembly

The shape of the tail-pipe burner discussed in this report was designed to accommodate fuselage installation in a specific airplane. The over-all length of the engine and the tail-pipe burner was approximately 21 feet. The tail-pipe-burner assembly, 11 feet, $7\frac{1}{4}$ inches long, consisted of three sections: (1) a diffuser section consisting of an annular diffuser and a conical diffuser separated by a short cylindrical section; (2) a burner section consisting of a converging conical section followed by a cylindrical section; and (3) a conical exhaust nozzle. The shell thickness was 0.38 inch for the diffuser and burner sections and 0.062 inch for the exhaust nozzle. Important dimensions of the assembly are shown in figure 2. The flame holder was located 6 inches upstream of the burner-section maximum diameter. The ratio of area at the plane of the flame holder to area at the turbine outlet was 1.65. A variable-area exhaust nozzle that would operate satisfactorily with tail-pipe burning was unavailable at the time of the investigation; a conical exhaust nozzle with a fixed outlet diameter of $20\frac{3}{32}$ inches was therefore used.

Three different fuel systems and three flame holders were investigated in the five configurations discussed in this report. Details and photographs of the fuel systems are shown in figures 3 and 4, flame-holder details and photographs are shown in figures 5 and 6. The combination of fuel system and flame holder used in each configuration is presented in the following table:

Configuration	Tail-pipe fuel system	Distance from fuel spray to flame holder (inches)	Flame holder	Flow area blocked by flame holder (percent)
A	I - Conical spray nozzle	$20\frac{5}{8}$	Medium two-V	29.1
B	II - Impinging-jet injectors	$23\frac{5}{8}$	Medium two-V	29.1
C	III - Impinging-jet injectors	$23\frac{5}{8}$	Medium two-V	29.1
D	III - Impinging-jet injectors	$23\frac{5}{8}$	Large two-V	30.3
E	III - Impinging-jet injectors	$23\frac{5}{8}$	Octagonal	18.6

Two other configurations also investigated are not discussed because the performance and the operational characteristics were unsatisfactory. In one of these configurations, the octagonal flame holder was used with fuel system I. In the other configuration, a semi-toroidal flame holder blocking 16.3 percent of the flow area was used with fuel system I combined with two rows of auxiliary conical spray nozzles located on the surface of the inner body of the annular diffuser. Each row contained 20 nozzles rated at 40 gallons per hour.

Fuel-systems. - Fuel system I (fig. 3(a)) consisted of a $13\frac{1}{4}$-inch-diameter ring of 20 conical spray nozzles rated at 40 gallons per hour at a differential pressure of 100 pounds per square inch. Fuel system II (fig. 3(b)) consisted of a set of 20 fuel injectors each containing two sets of impinging jets. The jets were so located that a reasonably uniform fuel-air mixture could be obtained over the flame holder and over-heating of the burner shell could be prevented by keeping the region near the pheriphery essentially free of fuel. In fuel system III (fig. 3(c)), five of the injectors of fuel system II were replaced by injectors having an additional set of jets at the center of the burner to improve flame stability. Fuel was injected in the downstream direction with each system.

Flame holders. - The three flame holders used in this investigation (figs. 5 and 6) are designated large two-V, medium two-V, and octagonal flame holders. These flame holders are identical to flame holders of the same designations described in reference 5.

The medium and large two-V flame holders each consisted of two annular-V-type gutters joined by four radial gutters between the annuli and supported by four radial struts secured to the tail-pipe skin. The octagonal flame holder had a semicircular cross section that was flat on the downstream side. This flame holder was designed to simulate the semitoroidal flame holder described in references 3 and 4.

Tail-pipe-burner cooling. - In order to provide a method of tail-pipe shell cooling that would be practical for flight installation, a liner made of 0.062-inch Inconel was installed inside the tail-pipe-burner shell, as shown in figures 2 and 6(a). The radial width of the space between the liner and the burner shell was approximately 1/2 inch. About 6 percent of the tail-pipe gas flowed through this space at approximately turbine-outlet temperature to cool the burner shell. In configurations A and B, the liner extended from the maximum diameter, 6 inches downstream of the flame holder, to the exhaust-nozzle inlet. In configurations C, D, and E, the liner was lengthened to extend from $2\frac{1}{2}$ inches upstream of the flame holder to the exhaust-nozzle inlet. More extensive experimental results of cooling-liner investigations, including methods of construction, are discussed in reference 5.

Ignition system. - In order to provide an ignition flame for the tail-pipe burner, a spark-ignition pilot burner similar to one described in reference 5 was installed, as shown in figure 2. A sheltered ignition region was provided at the downstream end of the diffuser inner body by a semispherical depression $6\frac{1}{4}$ inches in diameter and a 2-inch extension. A spark plug was installed through the extension and a 10-gallon-per-hour conical fuel-spray nozzle was installed in the center of the pilot burner. Additional fuel was supplied when necessary by a supplementary fuel system consisting of 20 conical spray nozzles rated at 40 gallons per hour and located on the surface of the diffuser inner body.

When failure of the spark plug rendered the pilot burner inoperative, it was necessary to use a stand-by method of ignition in which the tail-pipe fuel was ignited by means of a rapid engine acceleration of about 500 rpm.

Instrumentation

Pressure and temperature instrumentation was installed at several measuring stations in the engine and the tail-pipe burner. Cross sections of the measuring stations indicating the location of the instrumentation are shown in figure 7. Engine air flow was measured by the use of survey rakes mounted at the engine inlet, station 1. A complete pressure and temperature survey was obtained at the turbine outlet, station 6, and static-pressure measurements were made at the burner-section inlet, station 7. A total-pressure survey was obtained 1 inch upstream of the exhaust-nozzle outlet, station 8, with a water-cooled survey rake. Engine fuel flow and tail-pipe-burner fuel flow were measured by calibrated rotameters.

PROCEDURE

All tail-pipe-burner performance data were obtained with the engine operating at rated speed, 7700 rpm. Each tail-pipe-burner configuration was operated over a range of fuel-air ratios at the following simulated flight conditions:

Altitude (ft)	Average Flight Mach number, M_0	Configuration				
5,000	0.27	A	B	C	D	E
15,000	.27		B	C	D	
25,000	.27	A	B	C	D	E
25,000	.90	A	B	C	D	E
25,000	1.06		B	C	D	
35,000	.27	A	B	C	D	E
45,000	.26		B	C	D	E

Dry refrigerated air was supplied to the engine at the standard temperature for each flight condition except that the minimum temperature obtained was about -20° F. Total pressure at the engine inlet was regulated to correspond to the pressure that would exist with complete free-stream ram-pressure recovery at each flight condition.

An approximate check on the performance of each configuration was made at intervals during the investigation. If the check indicated that the performance of the configuration was relatively good at two or three flight conditions, and provided the operational characterisitics were satisfactory, further data were then obtained over a wide range of flight conditions. Data obtained with each configuration are given in table I.

Because all the data were obtained with a fixed-area exhaust nozzle, limiting turbine-outlet temperature could be obtained with each configuration at only one value of tail-pipe fuel-air ratio at each flight condition. The burner performance presented for each configuration therefore does not represent the performance that might be obtained with a variable-area exhaust nozzle. The use of a fixed-area exhaust nozzle, however, provided the most expeditious means of comparing the performance of the various modifications. Over-all performance is presented as a function of flight Mach number at a turbine-outlet temperature of 1650° R.

Augmented-thrust measurements were obtained from the balance scales and also from the pressure survey at the exhaust-nozzle outlet. The values of augmented thrust presented were determined from balance-scale measurements and therefore include the effect of losses in the exhaust jet. Exhaust-gas temperatures presented were calculated from total-pressure measurements at the exhaust-nozzle outlet by using an experimentally determined flow coefficient. The combustion efficiencies presented are based on these temperatures.

Symbols used in the report and methods of calculation used for the reduction of the data are presented in the appendix. The probable limits of error in the calculated values of jet thrust, exhaust-gas temperature, and combustion efficiency are $\pm 1\frac{1}{2}$, ± 3, and ± 5 percent, respectively. The jet-velocity coefficient, which accounts for velocity losses in the exhaust jet, was calculated from scale jet thrust and rake jet thrust and is presented in the appendix as a function of nozzle pressure ratio.

RESULTS AND DISCUSSION

Tail-pipe-burner performance variables, which include combustion efficiency and exhaust-gas temperature, and burner-inlet conditions, which include the burner-section-inlet velocity and the turbine-outlet total pressure and temperature, are presented as functions of tail-pipe fuel-air ratio. The tail-pipe fuel-air

ratio used herein is defined as the ratio of tail-pipe fuel flow to unburned air flow entering the tail-pipe burner, as shown in the appendix (equation (7)). Over-all performance at a turbine-outlet temperature of 1650° R is presented showing the variation of the augmented-thrust ratio, exhaust-gas temperature, tail-pipe combustion efficiency, and specific fuel consumption with flight Mach number. Combustion blow-out limits, which determine the operable range of tail-pipe fuel-air ratios, are presented as a function of altitude.

Comparison of Configurations

Fuel distribution. - The effect of changes in the fuel distribution on combustion efficiency and exhaust-gas total temperature is shown in figures 8 and 9, respectively. At all altitudes investigated, the more uniform mixture of fuel and air afforded by configurations B and C gave peak combustion efficiencies that were 0.03 to 0.13 higher than for configuration A, in which the fuel distribution was stratified. Improving the uniformity of the mixture also raised the tail-pipe fuel-air ratio at which the peak combustion efficiency occurred from a range of 0.020 to 0.025 for configuration A to a range of 0.035 to 0.040 for configurations B and C. At fuel-air ratios above 0.025, the combustion efficiency was as much as 0.05 higher with configuration C than with configuration B. The effect of fuel distribution on exhaust-gas total temperature (fig. 9) was similar to the effect on combustion efficiency. At fuel-air ratios above 0.030, the highest exhaust-gas total temperature at all altitudes was obtained with configuration C.

Flame holders. - The combined effect of flame-holder type and blocked area on combustion efficiency and exhaust-gas total temperature is shown in figures 10 and 11, respectively. At all altitudes the greater flame-holding surface afforded by configurations C and D, which had the two-V flame holders, resulted in peak combustion efficiencies 0.07 to 0.10 higher than for configuration E, which had the octagonal flame holder. Peak combustion efficiencies were obtained at tail-pipe fuel-air ratios from 0.035 to 0.043. Increasing the blocked area by 1.2 percent from the medium to the large two-V flame holder caused a variation of less than 0.02 in tail-pipe combustion efficiency. The effect of flame-holder changes on exhaust-gas total temperature (fig. 11) was similar to the effect on combustion efficiency. At all fuel-air ratios, the highest temperatures were obtained with configurations C and D at all altitudes.

Tail-Pipe-Burner Performance

Data for configuration C are presented in figures 12 to 15 to show the variation of tail-pipe-burner-inlet conditions with altitude and flight Mach number and to demonstrate the effect of the burner-inlet conditions on the combustion efficiency and exhaust-gas total temperature.

Effect of altitude.- As the tail-pipe fuel-air ratio was increased at each altitude, the burner-section-inlet velocity increased slightly, the turbine-outlet total temperature increased measurably, except at an altitude of 45,000 feet, and the turbine-outlet total pressure increased slightly (fig. 12). At a constant value of tail-pipe fuel-air ratio, increasing altitude from 5000 to 45,000 feet at a flight Mach number of 0.27 had no effect on burner-inlet velocity but reduced the turbine-outlet total temperature considerably and decreased the turbine-outlet total pressure approximately in proportion to the change in altitude pressure.

As the fuel-air ratio was increased at altitudes from 5000 to 25,000 feet, the combustion efficiency (fig. 13(a)) rapidly increased to a peak value and remained relatively constant over a range of tail-pipe fuel-air ratios from 0.030 to 0.045. This trend also existed at an altitude of 35,000 feet, although data were not obtained at the low fuel-air ratios. At an altitude of 45,000 feet, however, the combustion efficiency decreased steadily as the fuel-air ratio was increased from the minimum to maximum limits of operation. At a given tail-pipe fuel-air ratio, reducing the turbine-outlet pressure by increasing the altitude lowered the tail-pipe combustion efficiency; at turbine-outlet total pressures below 1000 pounds per square foot this effect was more pronounced than at higher pressures. At a fuel-air ratio of 0.036, the combustion efficiency (fig. 13(a)) was reduced from 0.83 to 0.72 when the turbine-outlet total pressure (fig. 12(c)) was decreased from 3300 to 1050 pounds per square foot by increasing the altitude from 5000 to 35,000 feet at a flight Mach number of 0.27; at the same fuel-air ratio, further decreasing the turbine-outlet total pressure from 1050 to 575 pounds per square foot by increasing the altitude from 35,000 to 45,000 feet lowered the combustion efficiency from 0.72 to 0.56.

The exhaust-gas total temperature (fig 13(b)) increased with tail-pipe fuel-air ratio at all altitudes except 45,000 feet. The effect of changes in altitude and the attendant changes in turbine-outlet total pressure on exhaust-gas total temperature was similar to the effect on combustion efficiency, with the highest temperatures for a given fuel-air ratio occurring at the highest turbine-outlet total pressure.

Effect of flight Mach number. - Tail-pipe-burner-inlet conditions are plotted against tail-pipe fuel-air ratio for a range of flight Mach numbers at an altitude of 25,000 feet in figure 14. As the flight Mach number was increased from 0.27 to 1.06 at a constant tail-pipe fuel-air ratio, the burner-section-inlet velocity remained constant, the turbine-outlet total temperature increased about 20° R, and the turbine-outlet total pressure increased approximately in proportion to the compressor-inlet total pressure. Varying the turbine-outlet total pressure by changing the flight Mach number at a constant fuel-air ratio had the same effect on the tail-pipe combustion efficiency and exhaust-gas total temperature (fig. 15) as variations in turbine-outlet total pressure due to changes in altitude (fig. 13). Reducing the turbine-outlet total pressure from about 3050 to 1700 pounds per square foot at a fuel-air ratio of 0.036 by changing the flight Mach number from 1.06 to 0.27 at an altitude of 25,000 feet (fig. 14(c)) reduced the tail-pipe combustion efficiency from 0.87 to 0.76 (fig. 15(a)) and decreased the exhaust-gas total temperature from 3000° to 2760° R (fig 15(b)).

Over-All Performance

Over-all performance obtained with configurations C and D, in which two-V flame holders were used, is presented in figure 16 for a turbine-outlet total temperature of 1650° R, the highest temperature at which data were available for cross-plotting. These results are compared with data from reference 5 for the performance obtained with the large two-V flame holder in a tail-pipe-burner assembly 8 feet, 9 inches long with a 29-inch-diameter cylindrical burner section. The 29-inch-diameter tail-pipe burner had the same exhaust-nozzle-outlet area as configurations C and D. The performance data presented are significant only for the size exhaust nozzle used in this investigation. With a larger exhaust-nozzle-outlet area at the same turbine-outlet temperature, higher thrust and exhaust-gas total temperature could be obtained; higher tail-pipe fuel-air ratios would be required; and the specific fuel consumption would also increase.

The augmented-thrust ratio is shown in figure 16(a) for a range of flight Mach numbers at an altitude of 25,000 feet. The augmented-thrust ratio is defined as the ratio of net thrust obtained with tail-pipe burning to the net thrust obtained with the standard-engine tail pipe. At a flight Mach number of 0.27, the augmented-thrust ratio of configurations C and D was 1.43 as compared with 1.45 for the 29-inch-diameter burner. At a flight Mach number of 0.90, the ratio had increased to 1.63 with configurations C and D as compared to 1.66 with the 29-inch-diameter

burner. The augmented-thrust ratio for configurations C and D was 1.64 at a flight Mach number of 1.06. The augmented-thrust ratio was lower for the converging conical tail-pipe burner than for the 29-inch-diameter cylindrical burner because the greater tail-pipe length and the converging shape of the burner section caused an increase in the total-pressure-loss ratio. At the operating conditions shown in figure 16, the pressure loss was about 0.085 of the turbine-outlet total pressure in configurations C and D as compared to 0.055 in the 29-inch-diameter cylindrical tail-pipe burner.

Exhaust-gas total temperature is shown in figure 16(b) for a range of flight Mach numbers at an altitude of 25,000 feet. The exhaust-gas total temperature with configurations C and D increased from 3030° R at a flight Mach number of 0.27 to 3150° R at a flight Mach number of 0.90, and to 3290° R at a flight Mach number of 1.06. Over the range of flight Mach numbers from 0.27 to 0.90, the temperature with the 29-inch-diameter burner increased from 3160 to 3290° R. Tail-pipe combustion efficiency at the aforementioned conditions is shown in figure 16(c). As the flight Mach number increased from 0.27 to 1.06, the combustion efficiency for configurations C and D increased from 0.74 to 0.89. Combustion efficiency for the 29-inch-diameter burner was approximately 0.81 at all flight Mach numbers from 0.27 to 0.90.

Specific fuel consumption based on net thrust is shown in figure 16(d) for a range of flight Mach numbers at an altitude of 25,000 feet. The specific fuel consumption for configurations C and D increased from 2.38 to 2.43 as the flight Mach number increased from 0.27 to 0.65 and decreased to 2.32 at a flight Mach number of 1.06. The specific fuel consumption obtained with the 29-inch-diameter burner increased from 2.38 to 2.48 as the flight Mach number increased from 0.27 to 0.90. The specific fuel consumption obtained with the standard-engine tail pipe increased from 1.18 to 1.33 as the flight Mach number was raised from 0.27 to 1.06.

Operational Characteristics

Combustion limits. - Tail-pipe fuel-air ratios at which combustion blow-out was encountered at altitudes from 5000 to 45,000 feet and a flight Mach number of 0.27 are shown for configurations C, D, and E in figure 17. At altitudes up to 35,000 feet, the range of tail-pipe fuel-air ratios over which the burner could be operated with the fixed-area exhaust nozzle extended from fuel-air ratios at which lean combustion blow-out occurred to fuel-air ratios at

which the turbine-outlet total temperature approached the limiting value. At altitudes above 35,000 feet, the range of operation extended from fuel-air ratios at which lean combustion blow-out occurred to fuel-air ratios at which rich combustion blow-out was encountered. At each altitude, the lean combustion limit occurred at about the same fuel-air ratio for all configurations. Fuel-air ratios for lean blow-out varied from about 0.021 at an altitude of 5000 feet to 0.014 at an altitude of 35,000 feet and 0.037 at an altitude of 45,000 feet. Rich combustion blow-out with configuration C was encountered at a tail-pipe fuel-air ratio of about 0.076 at altitudes of 37,500 to 45,000 feet; rich blow-out with configuration E occurred at fuel-air ratios of 0.064 and 0.053 at 35,000 and 42,500 feet, respectively. No rich combustion blow-out data were obtained for configuration D.

By use of a variable-area exhaust nozzle, the turbine-outlet temperature limit might be shifted to higher fuel-air ratios by increasing the exhaust-nozzle-outlet area. It is also possible that the lean blow-out limits would be shifted to lower fuel-air ratios by decreasing the exhaust-nozzle-outlet area and thereby maintaining higher pressures and temperatures at the tail-pipe-burner inlet.

Tail-pipe cooling. - Although the conical shape of the burner section complicated the fabrication and the installation of the cooling liner in this tail-pipe burner, the cooling provided compared satisfactorily with that obtained in the cylindrical burner section reported in reference 5. Measurements indicated that about 6 percent of the turbine-outlet gas passed through the 1/2-inch space between the burner shell and the cooling liner. By this method of cooling, shell temperatures lower than 1700° R were maintained at all flight conditions investigated. The temperature of the liner was considerably higher than the temperature of the shell; because it was not required to carry any appreciable stresses, the liner was able to withstand very high temperatures.

Several failures of the liner encountered in the early stages of the investigation indicated that the liner should not be rigidly secured to the burner shell because differential expansion between the two surfaces resulted in severe warpage of the liner. In subsequent phases of the investigation, methods of supporting the liner were found that allowed the liner to "float" inside the burner (reference 5). Occasional buckling of the liner was also caused by a pressure differential that forced the liner to collapse inwardly.

The maximum life of the cooling liners used in the configurations discussed was about 10 hours of tail-pipe burner operation. In later investigations, improvements in design and support of the liner extended the life to about 20 hours.

Tail-pipe fuel ignition. - The pilot burner in the diffuser inner body, which included a fuel spray nozzle and a spark plug, was operable at reduced engine speeds up to an altitude of 32,000 feet. Ignition of the tail-pipe fuel was accomplished by the pilot burner at 25,000 feet with an engine speed of 7000 rpm and at 30,000 feet with an engine speed of 6000 rpm. Use of the supplementary fuel system was not required for ignition at altitudes above 25,000 feet. The pilot-burner spark plug often failed from vibration and high temperature; consequently, this ignition system was unreliable.

The stand-by method of igniting the tail-pipe fuel, which consistently provided ignition at all flight conditions, consisted of a rapid engine acceleration of about 500 rpm resulting in a burst of flame through the turbine and into the tail pipe. Ignition of the tail-pipe fuel by this method occasionally resulted in blowout in the engine combustion chambers at an altitude of 45,000 feet. Although this method was satisfactory for experimental work, it is unsuitable for tactical use. From experience with this method, however, a reliable and suitable tail-pipe-burner ignition system was developed and is reported in reference 5.

SUMMARY OF RESULTS

The following results were obtained from an investigation of a tail-pipe burner with a converging conical burner section and a fixed-area exhaust nozzle on a J35-A-5 turbojet engine in the NACA Lewis altitude wind tunnel:

1. The most efficient burner performance and the widest range of operable fuel-air ratios were obtained with configurations in which fuel injectors that gave relatively uniform distribution of the tail-pipe fuel-air mixture were used with annular-V-gutter type flame holders blocking about 30 percent of the burner cross-sectional area.

2. With a given tail-pipe fuel-air ratio, lowering the turbine-outlet total pressure, either by an increase in altitude or by a decrease in flight Mach number, reduced the tail-pipe combustion efficiency and the exhaust-gas total temperature.

Tail-pipe combustion efficiency was adversely affected to a greater extent by reductions in turbine-outlet pressure below about 1000 pounds per square foot than at higher pressures.

3. At an altitude of 25,000 feet and with a turbine-outlet temperature of 1650° R, the ratio of augmented thrust to normal thrust increased from 1.43 at a flight Mach number of 0.27 to 1.64 at a flight Mach number of 1.06. Over the same range of flight Mach numbers, the exhaust-gas temperature increased from 3030° to 3290° R and the tail-pipe combustion efficiency increased from 0.74 to 0.89. The specific fuel consumption based on net thrust increased from 2.37 at a flight Mach number of 0.27 to 2.43 at a flight Mach number of 0.65 and then decreased to 2.32 at a flight Mach number of 1.06.

4. At a flight Mach number of 0.27, the operable range of tail-pipe fuel-air ratios narrowed as the altitude was increased above 35,000 feet. At 45,000 feet, the operating range of the best configuration was limited to fuel-air ratios between 0.037 and 0.076 by lean and rich blow-out limits.

5. The use of an internal cooling liner extending the full length of the burner section (approximately 60 in.) with a 1/2-inch space between the liner and the burner shell provided adequate shell cooling at all flight conditions investigated.

Lewis Flight Propulsion Laboratory,
National Advisory Committee for Aeronautics,
Cleveland, Ohio.

APPENDIX - CALCULATIONS

Symbols

A	cross-sectional area, sq ft
B	thrust scale reading, lb
C_d	flow (discharge) coefficient, ratio of effective flow area to measured area
C_j	jet-velocity coefficient, ratio of actual jet velocity to ideal jet velocity after expansion to free-stream static pressure
C_T	thermal-expansion ratio, ratio of hot-exhaust-nozzle-outlet area to cold-exhaust-nozzle-outlet area
D	external drag of installation, lb
D_r	drag of exhaust-nozzle survey rake, lb
F_j	jet thrust, lb
F_n	net thrust, lb
f/a	fuel-air ratio
g	acceleration due to gravity, 32.2 ft/sec^2
H	total enthalpy, Btu/lb
h_c	lower heating value of fuel, Btu/lb
M	Mach number
P	total pressure, lb/sq ft absolute
P_8'	total pressure at exhaust-nozzle survey station in standard-engine tail pipe, lb/sq ft absolute
p	static pressure, lb/sq ft absolute
R	gas constant, ft-lb/(lb)(^oR)
T	total temperature, ^oR

T_i	indicated temperature, °R
t	static temperature, °R
V	velocity, ft/sec
W_a	air flow, lb/sec
W_c	bearing cooling-air flow, lb/sec
W_f	fuel flow, lb/hr
W_f/F_n	specific fuel consumption based on total fuel flow and net thrust, lb/(hr)(lb thrust)
W_g	gas flow, lb/sec
γ	ratio of specific heats for gases
η_b	combustion efficiency
ρ	static density, slugs/cu ft

Subscripts:

a	air
e	engine
f	fuel
g	gas
j	jet
m	fuel manifold
s	scale
t	tail-pipe burner
x	inlet duct at labyrinth slip joint
0	free-stream conditions
1	engine inlet

3	engine combustion-chamber inlet
6	turbine outlet (diffuser inlet)
7	burner-section inlet, $8\frac{3}{4}$ inches upstream of flame-holder plane
8	exhaust-nozzle total-pressure survey plane, 1 inch upstream of outlet
9	exhaust-nozzle outlet

Methods of Calculation

Flight Mach number and airspeed. - Flight Mach number and equivalent airspeed were calculated from ram-pressure ratio by the following equations with complete pressure recovery at the engine inlet assumed:

$$M_0 = \sqrt{\frac{2}{\gamma_1 - 1}\left[\left(\frac{p_1}{p_0}\right)^{\frac{\gamma_1 - 1}{\gamma_1}} - 1\right]} \tag{1}$$

$$V_0 = M_0\sqrt{\gamma_1 g R T_1\left(\frac{p_0}{p_1}\right)^{\frac{\gamma_1 - 1}{\gamma_1}}} \tag{2}$$

The equivalent free-stream total temperature was assumed equal to the compressor-inlet indicated temperature. The use of this assumption introduces an error in airspeed of less than 1 percent.

Air flow. - Air flow at the engine inlet was determined from pressure and temperature measurements obtained with four survey rakes in the inlet annulus. The following equation was used for calculation of air flow:

$$W_{a,1} = p_1 A_1 \sqrt{\frac{2\gamma_1 g}{(\gamma_1 - 1)Rt_1}\left[\left(\frac{P_1}{p_1}\right)^{\frac{\gamma_1 - 1}{\gamma_1}} - 1\right]} \tag{3}$$

Bearing cooling air was bled from the compressor in a quantity approximately equal to the engine fuel flow. The air flow entering the engine combustion chamber was therefore calculated as follows:

$$W_{a,3} = W_{a,1} - W_c = W_{a,1} - \left(\frac{W_{f,e}}{3600}\right) \tag{4}$$

Temperatures. - Static temperatures were calculated from indicated temperatures by the adiabatic relation between temperature and pressure, using an impact recovery factor that had been determined as 0.85 for the type of thermocouple used:

$$t = \frac{T_i}{1 + 0.85\left[\left(\frac{P}{p}\right)^{\frac{\gamma - 1}{\gamma}} - 1\right]} \tag{5}$$

Tail-pipe gas flow. - The tail-pipe gas flow was determined by calculating the weight flow entering the tail-pipe burner, as follows:

$$W_g = W_{a,3} + \frac{W_{f,e} + W_{f,t}}{3600} \tag{6}$$

Tail-pipe fuel-air ratio. - The tail-pipe fuel-air ratio used herein is defined as the weight flow of fuel injected in the tail-pipe burner divided by the weight flow of unburned air entering the tail-pipe burner from the engine. Weight flow of unburned air was determined by assuming that the fuel injected in the engine was completely burned. By combining air flow, engine fuel flow, and tail-pipe fuel flow, the following equation for tail-pipe fuel-air ratio is obtained:

$$(f/a)_t = \frac{W_{f,t}}{3600\, W_{a,3} - \frac{W_{f,e}}{0.067}} \tag{7}$$

where 0.067 is the stoichiometric fuel-air ratio for the engine fuel.

Turbine-outlet temperature. - Because the temperature measurements at station 6 were unreliable when the tail-pipe burner was in operation, the turbine-outlet temperatures listed in table I were calculated by means of the following relation:

$$H_6 = \frac{W_{a,3} H_{a,1} + \frac{W_{f,e}}{3600} h_{c,e} \eta_{b,e}}{W_{a,3} + \frac{W_{f,e}}{3600}} \tag{8}$$

An engine combustion efficiency $\eta_{b,e}$ of approximately 98 percent at rated engine speed was determined from experiments with the standard engine using more reliable temperature instrumentation at the turbine outlet. After calculating H_6 by equation (8), turbine-outlet temperature T_6 was determined from H_6 and fuel-air ratio by use of enthalpy-temperature charts.

Burner-section-inlet velocity. - Velocity at the burner-section inlet was calculated by using static pressure measured at station 7, $8\frac{3}{4}$-inches upstream of the flame holder, and by assuming constant total pressure and total temperature from turbine outlet to burner-section inlet.

$$V_7 = \frac{W_g}{\rho_7 g A_7} = \frac{W_g R T_6}{p_7 A_7} \left(\frac{p_7}{P_6}\right)^{\frac{\gamma_6 - 1}{\gamma_6}} \tag{9}$$

Combustion efficiency. - Tail-pipe combustion efficiency was obtained by dividing the enthalpy rise through the tail-pipe burner by the heat content of the tail-pipe fuel.

$$\eta_{b,t} = \frac{3600 W_g \Delta H_t}{W_{f,t} h_{c,t}}$$

$$= \frac{3600 W_{a,3} H_a \Big]_{T_1}^{T_9} + W_{f,e} H_{f,e} \Big]_{T_m}^{T_9} - W_{f,e} h_{c,e} + W_{f,t} H_{f,t} \Big]_{T_m}^{T_9}}{W_{f,t} h_{c,t}} \tag{10}$$

The engine fuel was assumed to be burned completely in the engine; inasmuch as the engine combustion efficiency has been found to be approximately 98 percent, this assumption involves less than one-half of 1 percent error in the value of tail-pipe combustion efficiency. The enthalpy of the combustion products was determined from the hydrogen-carbon ratio of the fuels by the method explained in reference 6, in which dissociation is disregarded.

Exhaust-gas total temperature. - The total temperature of the exhaust gas was calculated from exhaust-nozzle outlet pressures and gas flow by means of the following equation:

$$T_9 = \frac{\gamma_9 g}{R}\left(\frac{C_d C_T A_9 p_9 M_9}{W_g}\right)^2\left(\frac{P_8}{p_9}\right)^{\frac{\gamma_9-1}{\gamma_9}} \qquad (11)$$

Exhaust-nozzle static pressure p_9 was determined by considering critical pressure ratio as follows:

when $\left(\frac{P_8}{p_0}\right) < \left(\frac{\gamma_9+1}{2}\right)^{\frac{\gamma_9}{\gamma_9-1}}$

$$p_9 = p_0 \quad \text{(subsonic flow)}$$

and when $\left(\frac{P_8}{p_0}\right) > \left(\frac{\gamma_9+1}{2}\right)^{\frac{\gamma_9}{\gamma_9-1}}$

$$p_9 = \frac{P_8}{\left(\frac{\gamma_9+1}{2}\right)^{\frac{\gamma_9}{\gamma_9-1}}} \quad \text{(sonic flow)}$$

Exhaust-nozzle-outlet Mach number M_9 was determined from jet Mach number M_j by assuming constant total pressure in the exhaust jet.

$$M_j^2 = \frac{2}{\gamma_9 - 1}\left[\left(\frac{P_8}{P_0}\right)^{\frac{\gamma_9 - 1}{\gamma_9}} - 1\right]$$

When $M_j < 1$, $M_9 = M_j$ (subsonic flow); when $M_j > 1$, $M_9 = 1$ (sonic flow) because the exhaust-nozzle outlet is the minimum area in the flow path.

The values of C_d and C_T for the exhaust nozzle used were determined from the following relations, which were experimentally obtained:

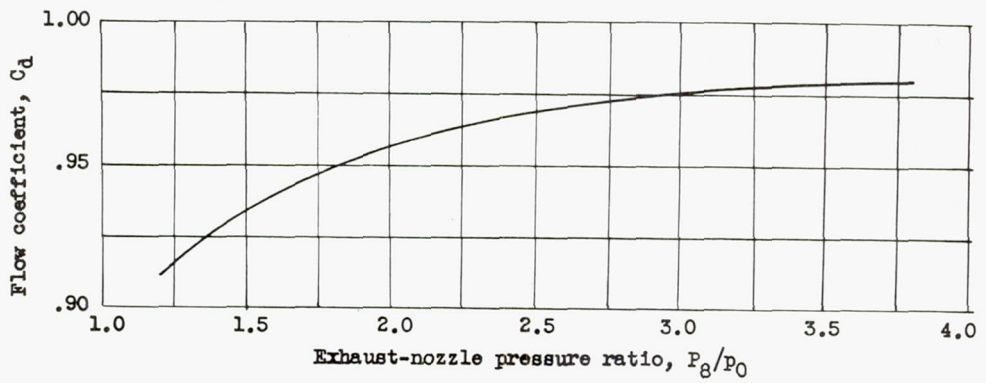

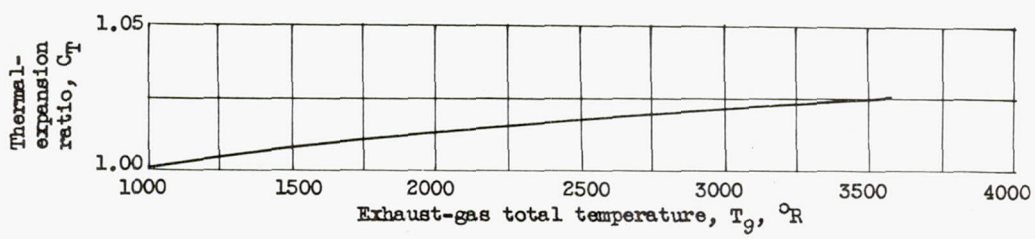

The ratio of specific heats γ_9 and the thermal-expansion ratio C_T were based on an estimated value of exhaust-gas temperature determined from the scale-thrust measurement.

Augmented thrust. - Actual jet thrust was determined from the balance-scale measurements by use of the following equation:

$$F_{j,s} = B + D + D_r + \frac{W_{a,x}V_x}{g} + A_x (p_x - p_0) \tag{12}$$

The last two terms of this expression represent momentum and pressure forces on the installation at the slip joint in the inlet-air duct. External drag of the installation was determined from experiments with a blind flange installed at the engine inlet to prevent air flow through the engine. Drag of the exhaust-nozzle survey rake was measured over a range of jet Mach numbers by a hydraulic-balance-piston mechanism.

Equivalent free-stream momentum of the inlet air was subtracted from scale jet thrust to determine net thrust as follows:

$$F_n = F_{j,s} - \frac{W_{a,1} V_0}{g} \tag{13}$$

Normal thrust. - The augmented-thrust ratio and the engine specific fuel consumption were based on the net thrust obtainable at rated engine speed with the standard-engine tail pipe. The standard-engine thrust was calculated from measurements of total pressure and temperature at the turbine outlet obtained during the progress of the tail-pipe-burning program.

$$F_n = \frac{\left(W_{a,3} + \frac{W_{f,e}}{3600}\right)}{g} C_j \sqrt{\frac{2\gamma}{\gamma-1} gRT_6 \left[1 - \left(\frac{p_0}{p_8'}\right)^{\frac{\gamma_6-1}{\gamma_6}}\right]} - \frac{W_{a,1} V_0}{g} \tag{14}$$

Experimental data indicated that the total-pressure loss through the standard tail pipe from station 6 to station 8 was approximately 0.01 P_6 at rated engine speed. The total pressure P_8' is therefore equal to 0.99 P_6. A jet-velocity coefficient C_j of 0.97 was used for the calculation of the results presented. This value of C_j was obtained from calibration of the engine with the standard-engine tail pipe and exhaust nozzle.

Rake jet thrust. - Jet thrust may be calculated from exhaust-nozzle-outlet pressure, assuming constant total pressure in the exhaust jet.

$$F_{j,9} = \frac{W_g}{g} V_j = \frac{W_g}{g} V_9 + C_d C_T A_9 (p_9 - p_0)$$

$$= C_d C_T A_9 \left[\gamma_9 p_9 M_9 + (p_9 - p_0)\right] \tag{15}$$

The terms on the right-hand side of equation (15) were determined in the same manner as for equation (11). Thus, the equation becomes as follows for subsonic and sonic flow, respectively:

When $M_j < 1$, $M_9 = M_j$, and $p_9 = p_0$,

$$F_{j,9} = C_d C_T A_9 \gamma_9 p_0 M_j \tag{15a}$$

When $M_j > 1$, $M_9 = 1$, and $p_9 = \dfrac{p_8}{\left(\dfrac{\gamma_9+1}{2}\right)^{\frac{\gamma_9}{\gamma_9-1}}}$,

$$F_{j,9} = C_d C_T A_9 \left[\frac{p_8(\gamma_9+1)}{\left(\dfrac{\gamma_9+1}{2}\right)^{\frac{\gamma_9}{\gamma_9-1}}} - p_0\right] \tag{15b}$$

Jet-velocity coefficient. - For the exhaust nozzle used, the jet-velocity coefficient may be expressed as the ratio of scale jet thrust (equation (12)) to rake jet thrust (equation (15))

$$C_j = \frac{\text{actual } V_j}{\text{ideal } V_j} = \frac{F_{j,s}}{F_{j,9}}$$

The relation of jet-velocity coefficient with tail-pipe burning to nozzle-pressure ratio is shown by the following curve, which was calculated from faired values of jet thrust:

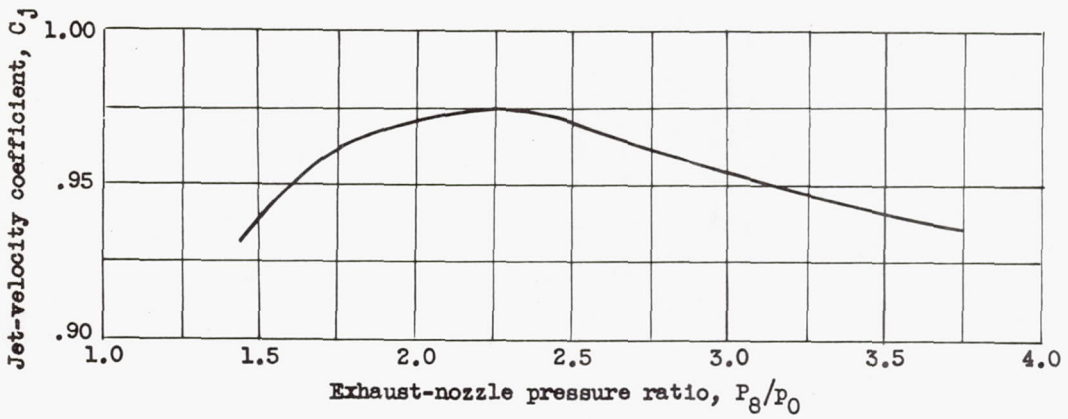

REFERENCES

1. Fleming, W. A., and Dietz, R. O.: Altitude-Wind-Tunnel Investigations of Thrust Augmentation of a Turbojet Engine. I - Performance with Tail-Pipe Burning. NACA RM E6I20, 1946.

2. Fleming, William A., and Golladay, Richard L.: Altitude-Wind-Tunnel Investigation of Thrust Augmentation of a Turbojet Engine. III - Performance with Tail-Pipe Burning in Standard-Size Tail Pipe. NACA RM E7F10, 1947.

3. Fleming, William A., and Wallner, Lewis E.: Altitude-Wind-Tunnel Investigation of Tail-Pipe Burning with a Westinghouse X24C-4B Axial-Flow Turbojet Engine. NACA RM E8J25e, 1948.

4. Lundin, Bruce T., Dowman, Harry W., and Gabriel, David S.: Experimental Investigation of Thrust Augmentation of a Turbojet Engine at Zero Ram by Means of Tail-Pipe Burning. NACA RM E6J21, 1947.

5. Conrad, E. William, and Prince, William R.: Altitude Performance and Operational Characteristics of 29-Inch-Diameter Burner with Several Fuel Systems and Flame Holders on J35 Turbojet Engine. NACA RM E9G08, 1949.

6. Turner, Richard L., and Lord, Albert M.: Thermodynamic Charts for the Computation of Combustion and Mixture Temperatures at Constant Pressure. NACA TN 1086, 1946.

TABLE I - PERFORMANCE DATA

Run	Altitude (ft)	Flight Mach number M_O	Free-stream pressure p_O (lb/sq ft abs.)	Engine-inlet total pressure P_1 (lb/sq ft abs.)	Engine-inlet total temperature T_1 (°R)	Engine fuel flow $W_{f,e}$ (lb/hr)	Tail-pipe fuel flow $W_{f,t}$ (lb/hr)	Jet thrust F_j (lb)	Net thrust F_n (lb)	Air flow W_a (lb/sec)
Configuration A										
1	5,000	0.280	1748	1842	482	2570	3020	3152	2536	67.33
2	5,000	.270	1752	1839	479	2990	3940	3860	3267	67.56
3	5,000	.280	1745	1841	480	3200	4700	4168	3547	67.58
4	5,000	.280	1755	1853	480	3770	7319	4964	4333	68.00
5	25,000	.305	775	828	459	1140	1310	1395	1082	31.48
6	25,000	.275	779	820	460	1400	1950	1894	1619	31.13
7	25,000	.275	775	816	451	1800	3520	2441	2165	31.47
8	25,000	.280	782	824	453	1880	5070	2532	2251	31.69
9	25,000	.270	779	818	454	1775	5600	2400	2132	31.36
10	25,000	.910	782	1334	481	1710	2450	3165	1791	48.88
11	25,000	.915	793	1363	477	2230	3630	4022	2605	50.27
12	25,000	.905	786	1339	479	2440	4540	4304	2926	49.22
13	25,000	.910	782	1334	477	2610	5600	4512	3136	49.19
14	25,000	.900	793	1341	476	2710	6340	4606	3232	49.52
15	35,000	.280	497	525	476	765	1000	964	788	19.10
16	35,000	.290	497	527	476	900	1500	1165	982	19.16
17	35,000	.315	500	535	477	1000	2000	1325	1125	19.42
18	35,000	.270	490	515	478	900	3020	1196	1031	18.66
Configuration B										
1	5,000	0.275	1748	1841	502	2540	4070	3165	2564	64.98
2	5,000	.265	1748	1836	495	2900	4520	3739	3154	65.55
3	5,000	.270	1759	1850	501	3500	5890	4629	4031	65.38
4	5,000	.270	1748	1838	504	3720	6527	4922	4335	64.64
5	15,000	.265	1194	1254	492	2030	3300	2710	2309	45.05
6	15,000	.255	1188	1243	483	2380	4000	3200	2815	45.39
7	15,000	.270	1191	1253	490	2540	4540	3460	3052	45.14
8	15,000	.270	1188	1248	486	2760	5300	3733	3330	45.26
9	25,000	.260	782	819	464	1180	2020	1952	1693	30.90
10	25,000	.270	782	822	465	1500	2500	2054	1785	30.93
11	25,000	.265	775	813	470	1710	3019	2332	2071	30.36
12	25,000	.285	769	814	466	1850	3630	2545	2259	30.57
13	25,000	.915	775	1330	508	1700	3240	3188	1841	46.44
14	25,000	.915	782	1344	508	2140	3800	3862	2498	46.94
15	25,000	.915	786	1354	505	2610	4800	4581	3202	47.50
16	25,000	.875	814	1339	510	2870	5957	4816	3512	46.58
17	25,000	.895	796	1339	503	3090	7353	5155	3815	47.18
18	25,000	1.080	762	1588	507	1900	3900	3921	2068	55.55
19	25,000	1.070	789	1621	503	2360	4170	4709	2829	57.12
20	25,000	1.065	782	1600	510	2840	5026	5348	3508	55.62
21	25,000	1.055	789	1595	504	3380	6527	6057	4227	56.07
22	35,000	.255	497	519	457	710	1010	863	706	19.55
23	35,000	.260	493	516	458	880	1500	1164	1003	19.37
24	35,000	.255	497	519	459	1070	2040	1473	1316	19.46
25	35,000	.275	486	512	456	1140	2350	1572	1402	19.32
26	45,000	.280	309	326	500	520	1070	631	526	11.20
27	45,000	.255	309	323	503	560	1490	679	585	11.03
28	45,000	.275	298	314	500	540	1800	688	588	10.78
Configuration C										
1	5,000	0.270	1752	1843	519	2500	3870	3053	2466	63.07
2	5,000	.255	1752	1835	514	2790	4120	3510	2952	63.40
3	5,000	.270	1766	1858	514	3180	5000	4155	3561	64.19
4	5,000	.265	1759	1846	514	3600	6111	4719	4145	63.79
5	15,000	.270	1188	1249	474	2165	3410	2919	2512	46.28
6	15,000	.275	1184	1247	475	2440	4020	3300	2885	46.12
7	15,000	.270	1188	1250	477	2650	4620	3605	3194	46.09
8	15,000	.260	1188	1245	481	2800	5140	3818	3425	45.61

OBTAINED WITH TAIL-PIPE BURNING

Specific fuel consumption $(W_{f,e}+W_{f,t})/F_n$ (lb/(hr)(lb thrust))	Total fuel-air ratio f/a	Tail-pipe fuel-air ratio $(f/a)_t$	Tail-pipe combustion efficiency $\eta_{b,t}$	Turbine-outlet total pressure P_6 (lb/sq ft abs.)	Turbine-outlet total temperature T_6 ($^\circ$R)	Burner-section-inlet static pressure p_7 (lb/sq ft abs.)	Exhaust-nozzle total pressure P_8 (lb/sq ft abs.)	Exhaust-gas total temperature T_9 ($^\circ$R)	Run
Configuration A									
2.204	0.0233	0.0150	0.602	2917	1246	2691	2702	1756	1
2.121	.0288	.0202	.699	3149	1349	2926	2909	2100	2
2.227	.0329	.0245	.693	3271	1414	3053	3010	2266	3
2.559	.0460	.0398	.613	3584	1560	3361	3286	2646	4
2.264	.0219	.0138	.535	1309	1189	1195	1209	1624	5
2.069	.0303	.0218	.694	1468	1353	1358	1344	2137	6
2.457	.0477	.0418	.632	1686	1568	1581	1534	2718	7
3.088	.0620	.0606	.474	1733	1610	1628	1583	2776	8
3.459	.0664	.0665	.393	1680	1563	1571	1536	2624	9
2.323	.0239	.0165	.572	2010	1187	1848	1844	1729	10
2.250	.0328	.0250	.696	2359	1354	2197	2164	2246	11
2.386	.0400	.0330	.633	2433	1454	2277	2225	2450	12
2.618	.0471	.0415	.566	2510	1520	2363	2290	2573	13
2.800	.0515	.0471	.548	2584	1542	2433	2353	2666	14
2.240	.0260	.0177	.587	850	1278	782	784	1856	15
2.444	.0352	.0276	.524	912	1402	845	832	2124	16
2.667	.0435	.0372	.544	995	1489	918	899	2426	17
3.802	.0592	.0574	.368	952	1425	886	872	2371	18
Configuration B									
2.578	0.0286	0.0211	0.544	2907	1282	2708	2725	1908	1
2.352	.0318	.0239	.665	3094	1362	2908	2893	2186	2
2.329	.0405	.0329	.798	3465	1550	3274	3208	2754	3
2.364	.0447	.0378	.806	3562	1621	3364	3290	2954	4
2.308	.0333	.0255	.706	2175	1385	2045	2027	2297	5
2.266	.0396	.0320	.746	2348	1511	2217	2175	2632	6
2.320	.0443	.0374	.777	2456	1584	2326	2262	2873	7
2.420	.0503	.0448	.767	2558	1664	2430	2357	3096	8
1.890	.0291	.0219	.506	1343	1230	1243	1258	1840	9
2.241	.0365	.0287	.713	1540	1420	1443	1422	2427	10
2.283	.0440	.0370	.706	1629	1565	1533	1484	2735	11
2.426	.0506	.0453	.703	1711	1642	1604	1559	2971	12
2.683	.0299	.0232	.542	2001	1239	1855	1858	1932	13
2.378	.0356	.0283	.732	2284	1404	2146	2113	2433	14
2.314	.0440	.0373	.828	2555	1574	2420	2354	2944	15
2.513	.0535	.0491	.804	2670	1699	2541	2463	3302	16
2.737	.0626	.0613	.731	2794	1758	2653	2572	3465	17
2.805	.0293	.0230	.510	2330	1199	2150	2162	1848	18
2.308	.0321	.0249	.712	2634	1319	2467	2449	2246	19
2.242	.0399	.0326	.890	2905	1509	2751	2695	2857	20
2.344	.0499	.0443	.954	3236	1668	3074	2996	3425	21
2.436	.0247	.0171	.508	826	1184	761	770	1685	22
2.373	.0346	.0270	.626	924	1358	861	855	2216	23
2.363	.0451	.0387	.673	1031	1533	970	948	2705	24
2.489	.0511	.0460	.659	1065	1609	1007	974	2897	25
3.023	.0400	.0335	.468	543	1414	506	502	2186	26
3.504	.0524	.0486	.383	556	1493	519	512	2331	27
3.980	.0611	.0598	.280	533	1475	498	491	2199	28
Configuration C									
2.583	0.0283	0.0207	0.459	----	1300	----	2637	1828	1
2.341	.0307	.0225	.704	3049	1380	2856	2829	2206	2
2.297	.0359	.0278	.794	3297	1486	3102	3045	2558	3
2.343	.0429	.0356	.837	3456	1609	3322	3234	2936	4
2.219	.0339	.0259	.722	2261	1399	2131	2090	2341	5
2.239	.0395	.0317	.768	2408	1509	2281	2215	2651	6
2.276	.0445	.0375	.795	2526	1591	2399	2321	2914	7
2.318	.0491	.0432	.811	2595	1667	2468	2385	3135	8

TABLE I - PERFORMANCE DATA OBTAINED

Run	Altitude (ft)	Flight Mach number M_O	Free-stream pressure p_O (lb/sq ft abs.)	Engine-inlet total pressure P_1 (lb/sq ft abs.)	Engine-inlet total temperature T_1 (°R)	Engine fuel flow $W_{f,e}$ (lb/hr)	Tail-pipe fuel flow $W_{f,t}$ (lb/hr)	Jet thrust F_j (lb)	Net thrust F_n (lb)	Air flow W_a (lb/sec)
Configuration C - Concluded										
9	25,000	0.280	782	825	458	1180	2100	1516	1234	31.40
10	25,000	.275	779	820	456	1520	2480	2076	1800	31.37
11	25,000	.270	789	830	455	1740	2990	2349	2072	31.79
12	25,000	.275	779	821	458	1920	3670	2636	2357	31.26
13	25,000	.885	779	1299	503	1870	3210	3386	2097	45.75
14	25,000	.885	775	1287	496	2150	3660	3862	2583	45.89
15	25,000	.880	779	1292	497	2510	4500	4397	3116	45.99
16	25,000	.890	782	1306	501	2660	4990	4571	3271	46.19
17	25,000	.870	782	1282	498	2810	5470	4634	3379	45.55
18	25,000	1.065	775	1585	496	2605	4380	5070	3229	56.51
19	25,000	1.060	789	1605	499	2720	4600	5161	3306	56.95
20	25,000	1.060	779	1582	499	2925	5100	5471	3645	56.10
21	25,000	1.060	782	1590	502	3370	6451	6057	4223	56.11
22	35,000	.270	497	523	443	1060	1810	1446	1272	20.20
23	35,000	.285	490	518	444	1180	2200	1588	1409	19.93
24	35,000	.285	493	521	442	1300	3020	1766	1585	20.14
25	45,000	.270	305	321	484	580	1140	703	601	11.35
26	45,000	.280	309	326	482	625	1700	777	670	11.59
27	45,000	.255	305	319	481	610	2050	754	658	11.36
Configuration D										
1	5,000	0.270	1748	1837	520	2970	4500	3734	3139	62.72
2	5,000	.280	1748	1844	523	3405	5590	4412	3812	62.63
3	5,000	.265	1752	1840	519	3680	6441	4788	4212	62.94
4	15,000	.280	1190	1255	484	2195	3525	2966	2545	45.67
5	15,000	.275	1190	1253	481	2475	4050	3344	2929	45.89
6	15,000	.270	1190	1252	481	2570	4400	3500	3089	45.86
7	15,000	.285	1188	1256	479	2680	4750	3664	3233	46.16
8	25,000	.270	775	815	460	1550	2510	2151	1880	30.94
9	25,000	.280	786	829	459	1760	3000	2389	2106	31.52
10	25,000	.275	775	816	464	1900	3570	2568	2286	30.80
11	25,000	.915	786	1356	509	2450	4220	4345	2966	47.26
12	25,000	.915	786	1356	517	2570	4640	4469	3100	46.57
13	25,000	.915	779	1337	512	2660	5100	4602	3252	46.32
14	25,000	1.060	789	1602	520	2550	4350	4847	3028	54.70
15	25,000	1.065	786	1604	523	2940	5250	5331	3509	54.51
16	25,000	1.060	793	1610	515	3010	5400	5495	3658	55.51
17	35,000	.270	497	523	455	800	1370	1058	886	19.76
18	35,000	.270	497	523	456	920	1610	1239	1067	19.72
19	35,000	.280	497	525	458	1120	1990	1528	1349	19.72
20	35,000	.260	497	521	458	1200	2350	1620	1455	19.57
21	45,000	.265	302	317	471	675	1380	836	736	11.50
22	45,000	.265	302	317	474	700	1820	847	747	11.42
23	45,000	.245	302	315	476	700	2200	857	765	11.31
Configuration E										
1	5,000	0.257	1741	1823	517	2380	4040	2786	2233	62.57
2	5,000	.273	1752	1845	515	2870	4910	3591	2996	63.56
3	5,000	.267	1752	1842	509	3380	6000	4398	3813	64.16
4	5,000	.276	1752	1847	505	3760	7305	4996	4390	64.78
5	25,000	.270	782	823	453	1160	2130	1502	1227	31.66
6	25,000	.267	782	822	454	1400	2510	1928	1656	31.52
7	25,000	.915	780	1341	512	1580	3420	2940	1583	46.45
8	25,000	.911	789	1350	505	2140	4170	3826	2459	47.37
9	25,000	.917	780	1342	508	2560	5180	4487	3125	46.83
10	25,000	.908	786	1340	497	2860	6267	4845	3483	47.68
11	35,000	.273	490	516	443	1070	2190	1493	1320	19.92
12	35,000	.263	490	514	442	1170	2690	1611	1445	19.88
13	35,000	.263	490	514	443	1070	3500	1514	1348	19.84
14	40,000	.278	385	406	486	740	1990	989	856	14.41
15	42,500	.257	344	360	489	600	1670	720	611	12.72
16	45,000	.243	309	322	490	520	1190	645	553	11.27

WITH TAIL-PIPE BURNING - Concluded

Specific fuel consumption $(W_{f,e}+W_{f,t})/F_n$ (lb/(hr)(lb thrust)	Total fuel-air ratio f/a	Tail-pipe fuel-air ratio $(f/a)_t$	Tail-pipe combustion efficiency $\eta_{b,t}$	Turbine-outlet total pressure P_6 (lb/sq ft abs.)	Turbine-outlet total temperature T_6 (°R)	Burner-section-inlet static pressure p_7 (lb/sq ft abs.)	Exhaust-nozzle total pressure P_8 (lb/sq ft abs.)	Exhaust-gas total temperature T_9 (°R)	Run
Configuration C - Concluded									
2.658	0.0293	0.0223	0.457	1351	1208	1259	1259	1776	9
2.222	.0359	.0281	.704	1555	1410	1463	1428	2382	10
2.283	.0419	.0346	.754	1694	1527	1602	1546	2724	11
2.372	.0506	.0450	.736	1755	1649	1674	1610	3043	12
2.422	.0312	.0239	.673	2104	1311	1969	1940	2163	13
2.249	.0356	.0281	.768	2269	1418	2140	2086	2484	14
2.250	.0430	.0360	.814	2465	1558	2339	2259	2891	15
2.339	.0468	.0405	.818	2547	1622	2424	2341	3061	16
2.450	.0513	.0461	.789	2583	1688	2460	2365	3196	17
2.163	.0348	.0271	.795	2768	1404	2609	2548	2485	18
2.214	.0361	.0286	.842	2859	1431	2701	2637	2618	19
2.202	.0403	.0330	.839	2937	1516	2779	2698	2810	20
2.326	.0495	.0437	.892	3202	1664	3041	2947	3309	21
2.256	.0401	.0326	.712	1038	1476	977	954	2570	22
2.399	.0479	.0418	.718	1091	1599	1033	1000	2894	23
2.726	.0607	.0586	.619	1161	1700	1103	1059	3123	24
2.862	.0427	.0362	.566	580	1483	543	530	2444	25
3.470	.0566	.0537	.410	604	1534	566	552	2486	26
4.042	.0660	.0660	.328	610	1530	552	540	2424	27
Configuration D									
2.380	0.0335	0.0253	0.741	3134	1448	2952	2894	2384	1
2.360	.0405	.0328	.817	3384	1575	3194	3108	2801	2
2.403	.0454	.0385	.801	3510	1649	3325	3227	2990	3
2.248	.0352	.0273	.727	2291	1425	2155	2096	2409	4
2.228	.0401	.0323	.777	2426	1534	2296	2222	2696	5
2.256	.0429	.0356	.806	2504	1570	2365	2287	2857	6
2.298	.0455	.0386	.783	2543	1606	2413	2331	2932	7
2.160	.0370	.0291	.747	1571	1442	1480	1440	2499	8
2.260	.0427	.0353	.758	1687	1552	1597	1542	2760	9
2.393	.0502	.0445	.749	1738	1659	1650	1589	3049	10
2.249	.0398	.0323	.832	2488	1516	2343	2274	2788	11
2.326	.0437	.0368	.854	2542	1590	2396	2324	2991	12
2.386	.0473	.0412	.824	2587	1627	2443	2365	3107	13
2.279	.0355	.0279	.818	2756	1437	2588	2516	2574	14
2.334	.0424	.0353	.944	3004	1568	2839	2753	3094	15
2.299	.0427	.0357	.903	3026	1568	2873	2781	3042	16
2.449	.0309	.0235	.515	889	1269	829	819	1921	17
2.371	.0361	.0287	.647	967	1375	906	885	2302	18
2.305	.0445	.0376	.730	1064	1566	1005	971	2786	19
2.440	.0512	.0460	.717	1101	1649	1043	1007	3021	20
2.792	.0505	.0452	.562	617	1619	582	562	2698	21
3.373	.0623	.0611	.532	649	1660	612	589	2954	22
3.791	.0725	.0748	.381	628	1672	592	573	2755	23
Configuration E									
2.875	0.0288	0.0216	0.424	2782	1275	2590	2595	1782	1
2.597	.0344	.0269	.618	3094	1400	2900	2859	2242	2
2.460	.0413	.0340	.709	3367	1540	3175	3105	2655	3
2.520	.0482	.0424	.740	3595	1630	3402	3315	2975	4
2.681	.0292	.0224	.382	1332	1195	1234	1238	1670	5
2.361	.0349	.0276	.559	1480	1335	1382	1363	2127	6
3.158	.0301	.0241	.455	1956	1190	1813	1803	1802	7
2.566	.0375	.0307	.666	2320	1390	2170	2122	2409	8
2.477	.0466	.0407	.772	2545	1565	2399	2332	2960	9
2.620	.0540	.0500	.739	2687	1650	2548	2470	3170	10
2.470	.0461	.0402	.623	1042	1495	980	957	2635	11
2.671	.0548	.0511	.555	1078	1590	1017	987	2783	12
3.390	.0650	.0646	.396	1041	1500	980	961	2574	13
3.189	.0534	.0498	.425	734	1490	686	678	2432	14
3.715	.0503	.0463	.364	617	1410	576	574	2201	15
3.092	.0427	.0370	.347	523	1400	488	490	2024	16

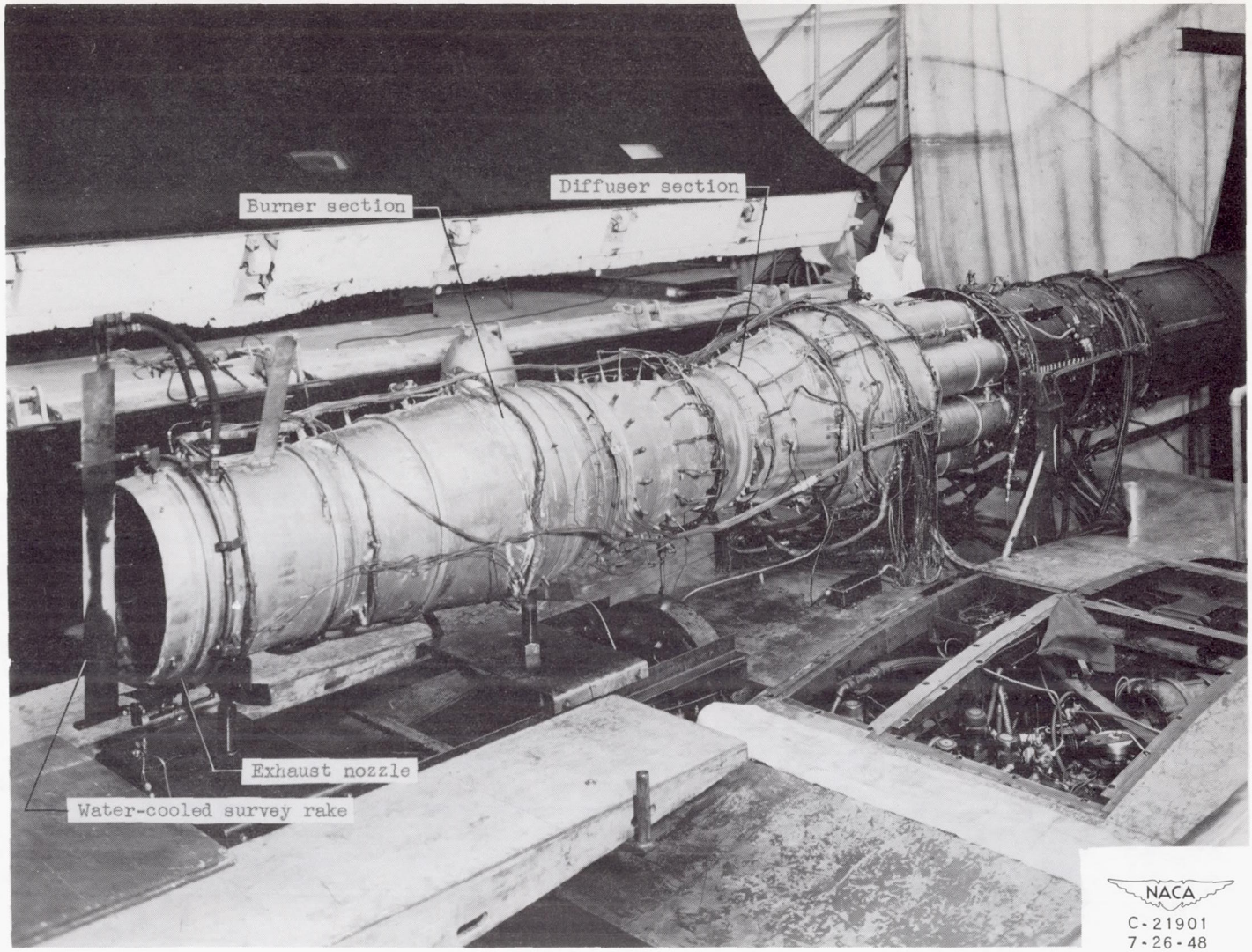

Figure 1. - Installation of engine and tail-pipe-burner assembly in altitude wind tunnel.

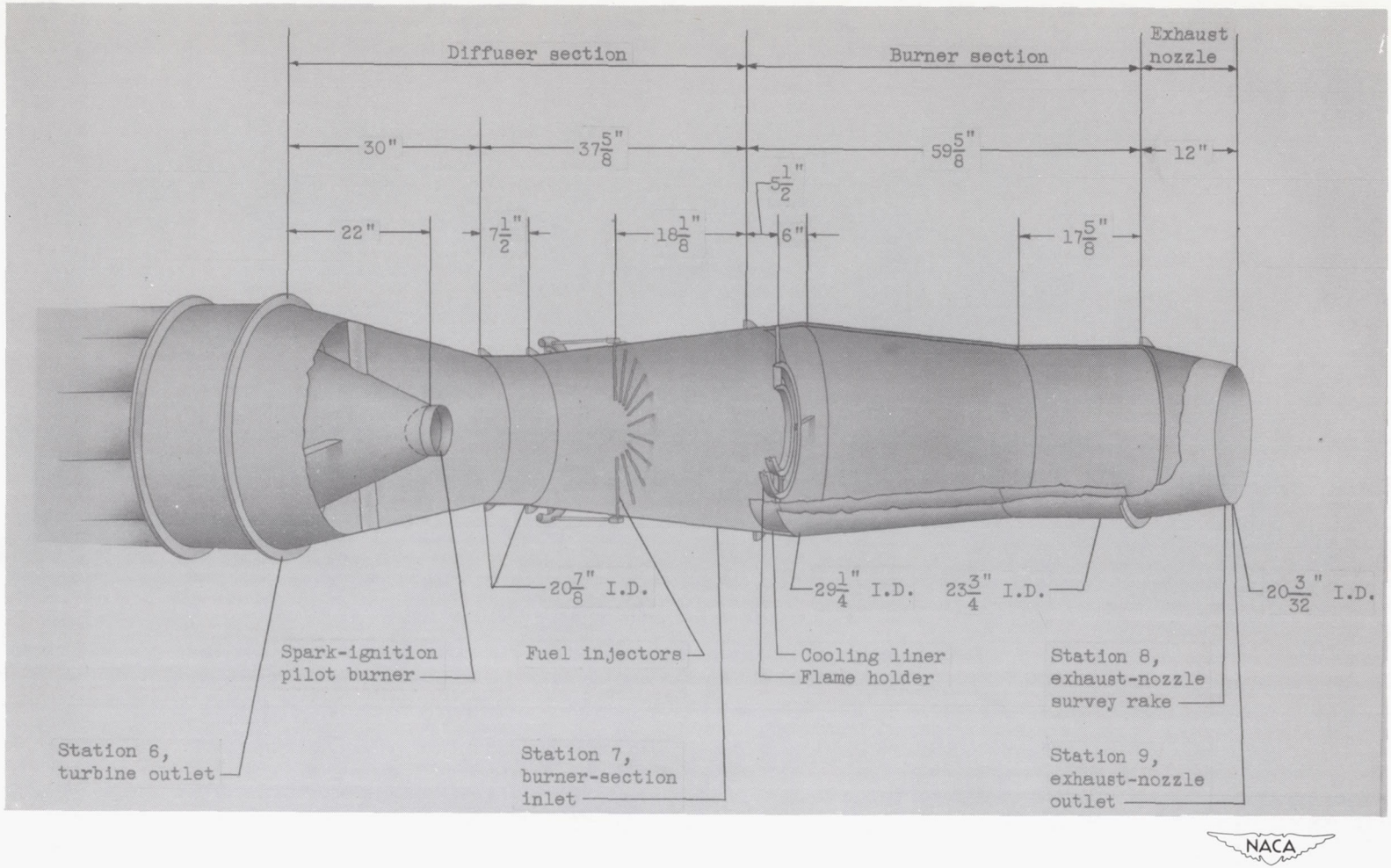

Figure 2. - Schematic diagram of tail-pipe-burner assembly.

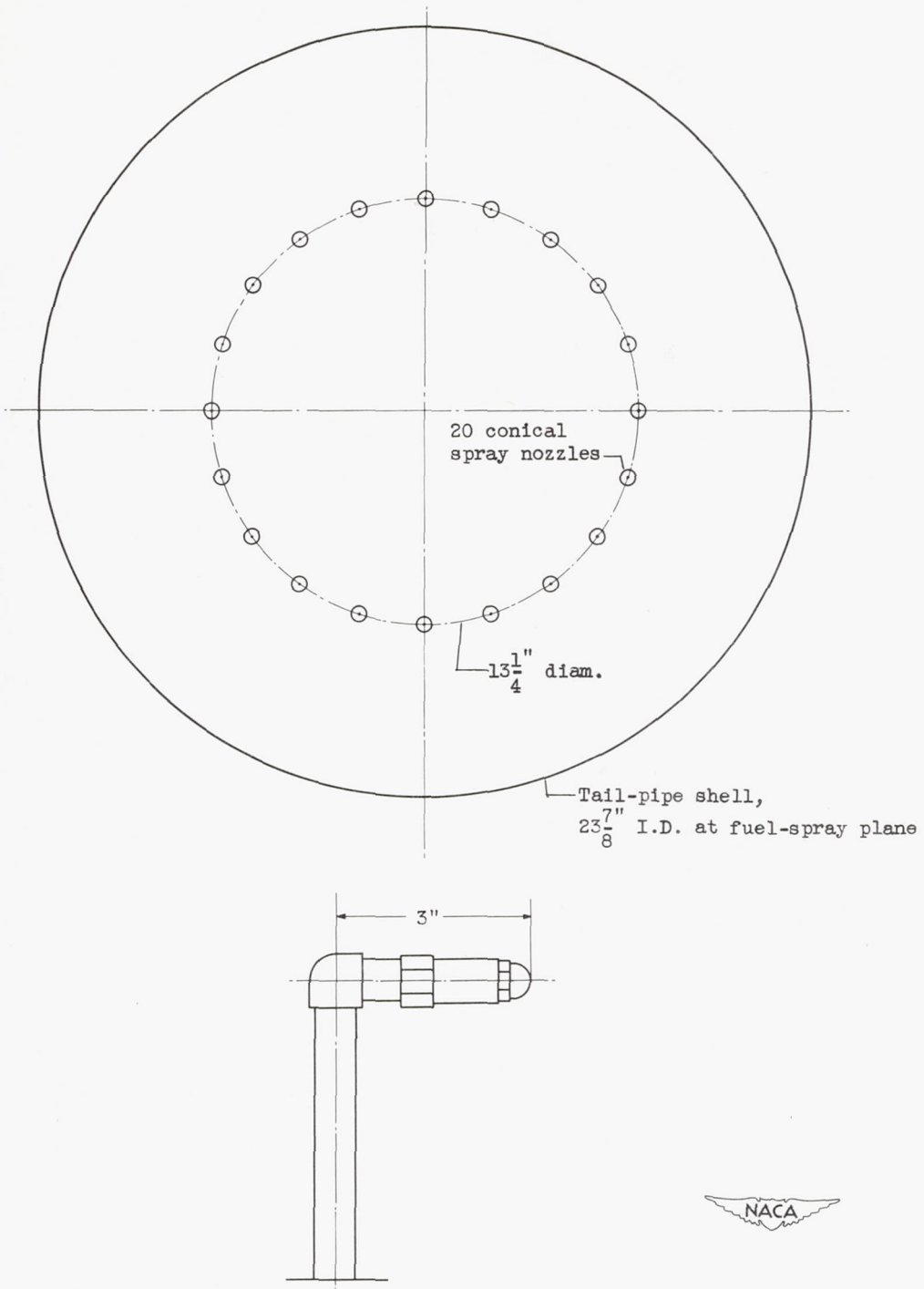

(a) Fuel system I; fuel-injection pattern with 40 gallon-per-hour conical spray nozzles.

Figure 3. - Schematic diagrams of fuel systems.

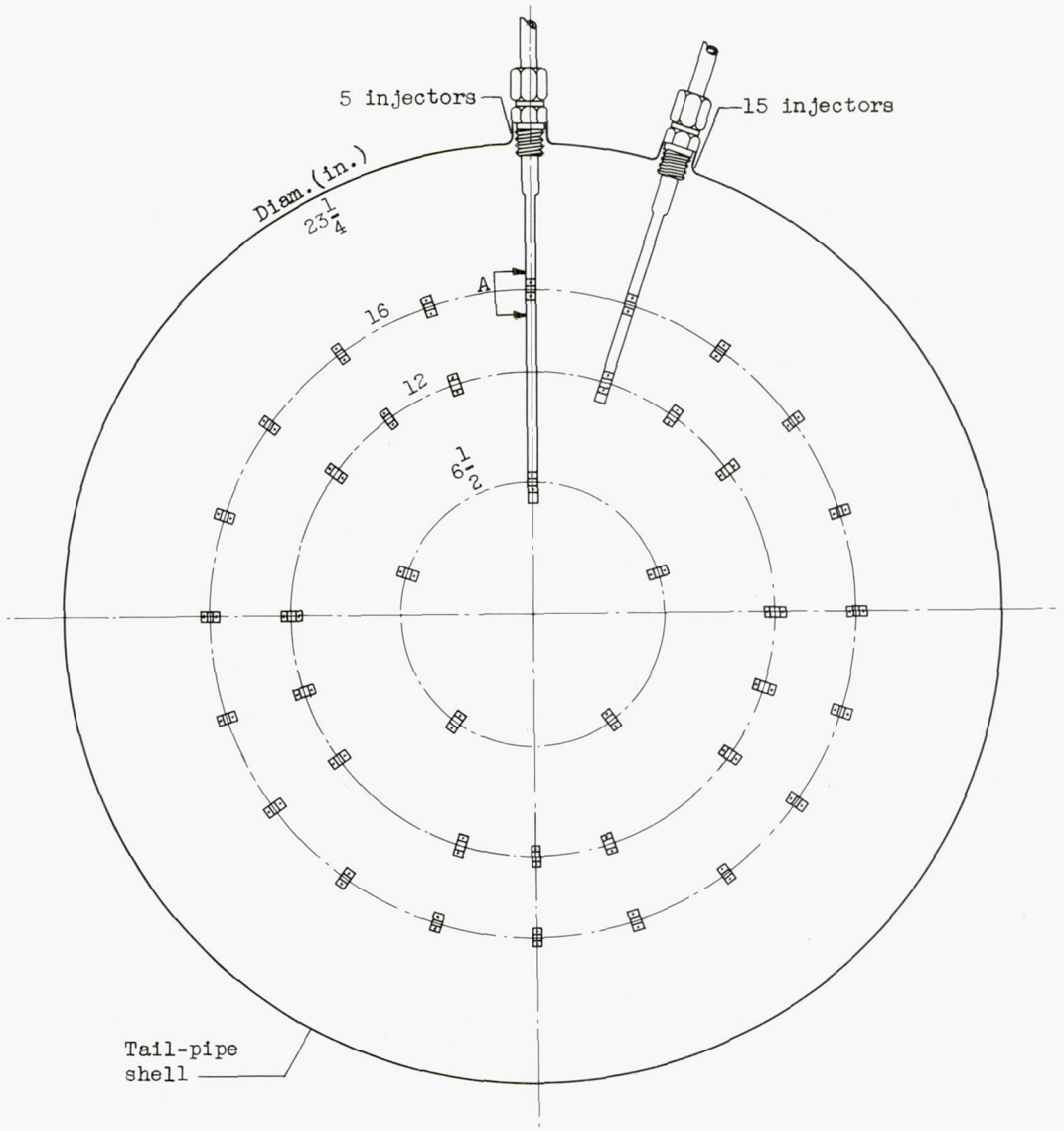

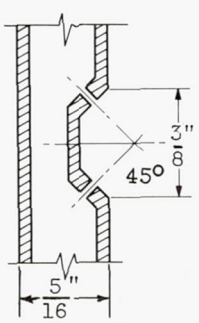

Detail A, impinging jet

Diameter (in.)	Number of jets	Diameter of holes (in.)
16	20	0.045
12	15	0.040
6 1/2	5	0.040

NACA

(b) Fuel system II; fuel-injection pattern and details of impinging-jet fuel injectors.

Figure 3. - Continued. Schematic diagrams of fuel systems.

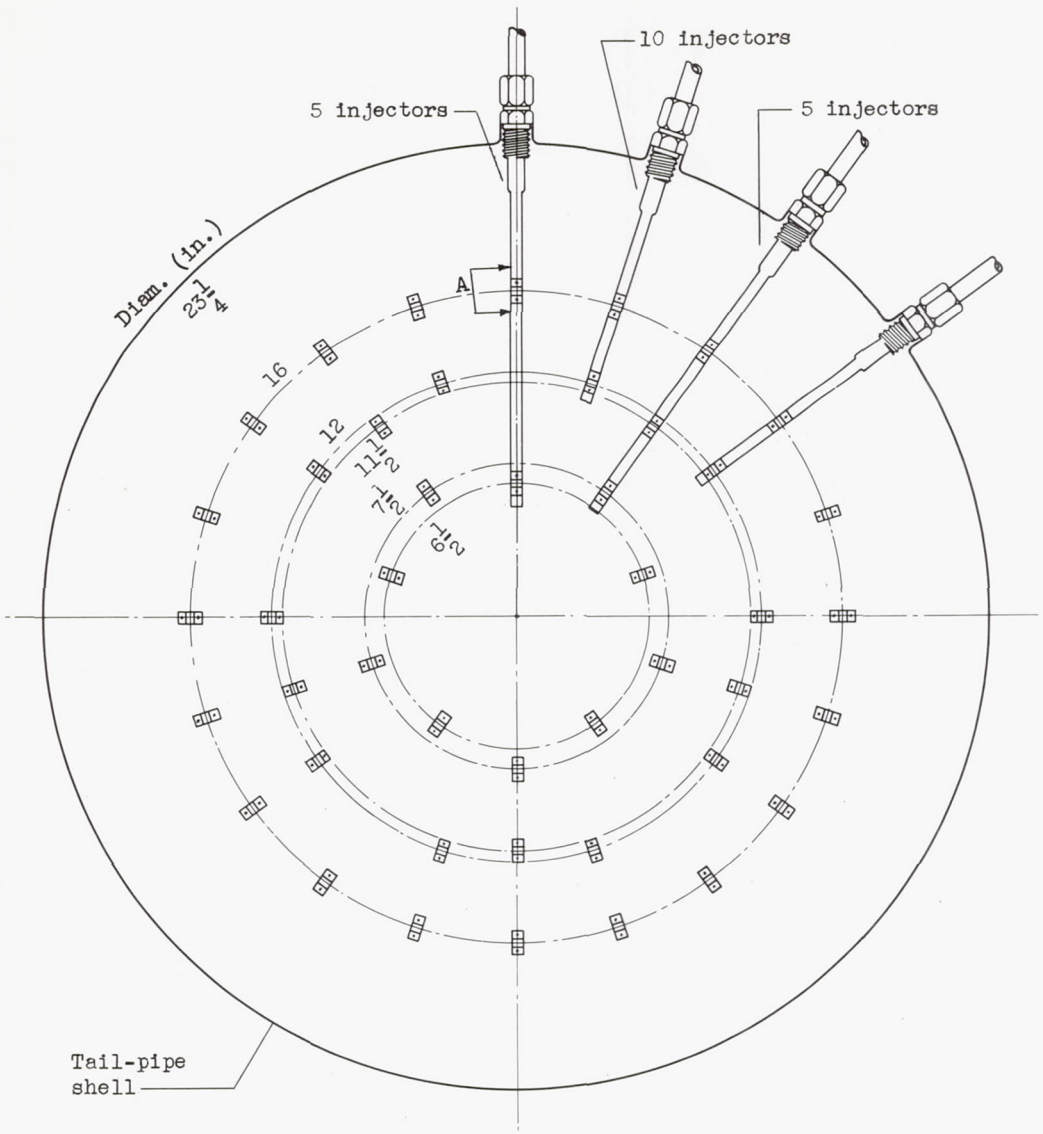

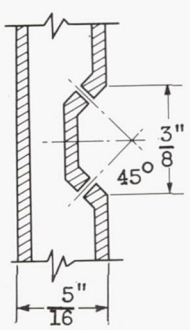

Detail A, impinging jet

Diameter (in.)	Number of jets	Diameter of holes (in.)
16	20	0.045
12	10	0.040
11 1/2	5	.045
7 1/2	5	0.045
6 1/2	5	.045

(c) Fuel system III; fuel-injection pattern and details of impinging-jet fuel injectors.

Figure 3. - Concluded. Schematic diagrams of fuel systems.

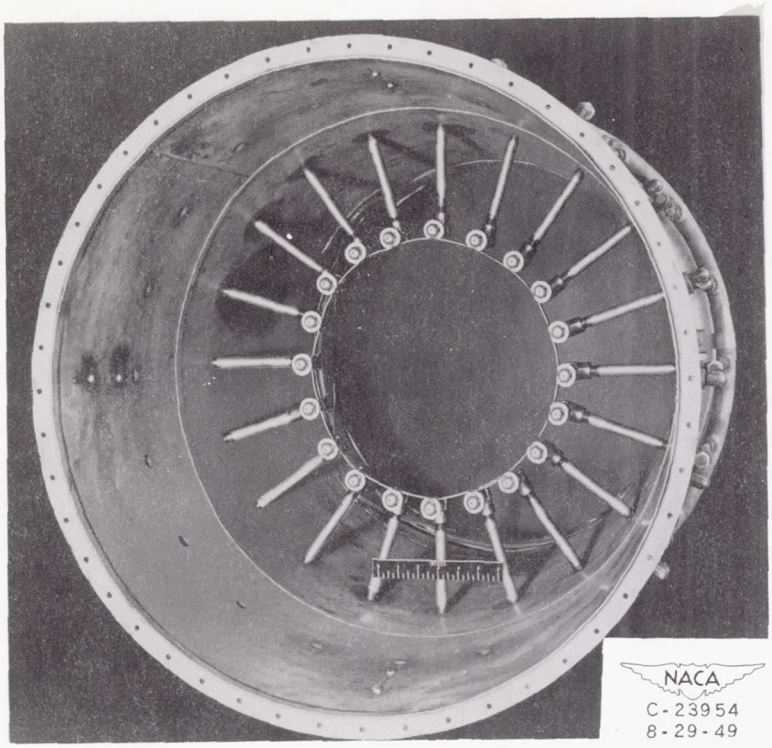

(a) Fuel system I.

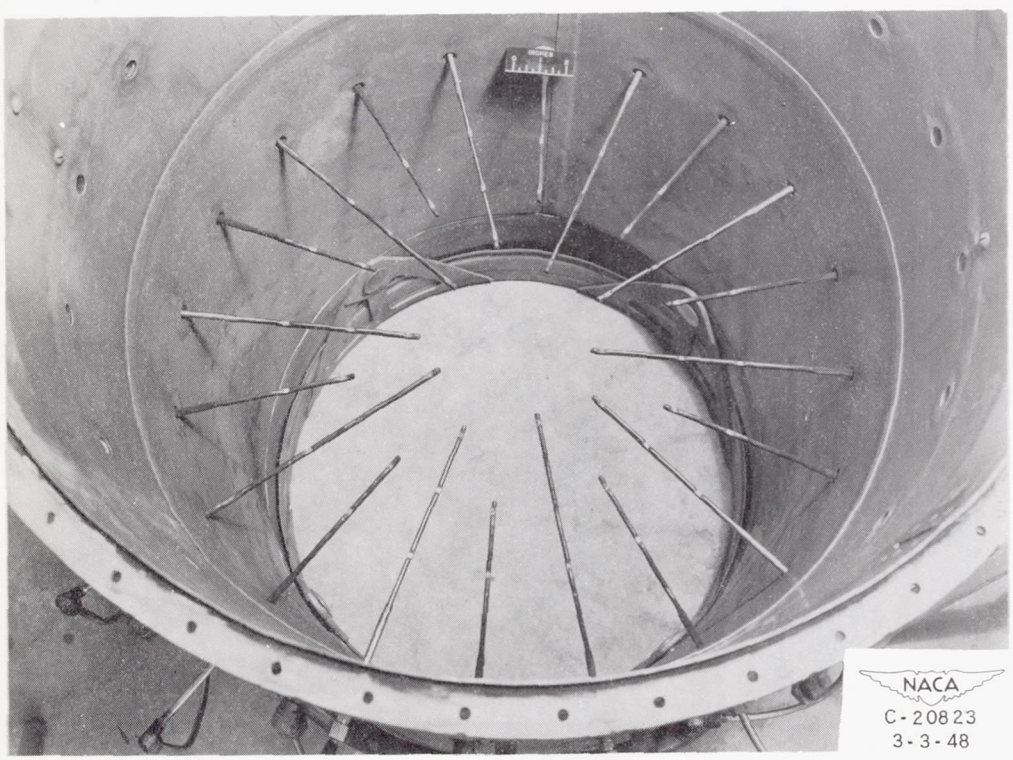

(b) Fuel system III.

Figure 4. - Fuel systems; looking upstream.

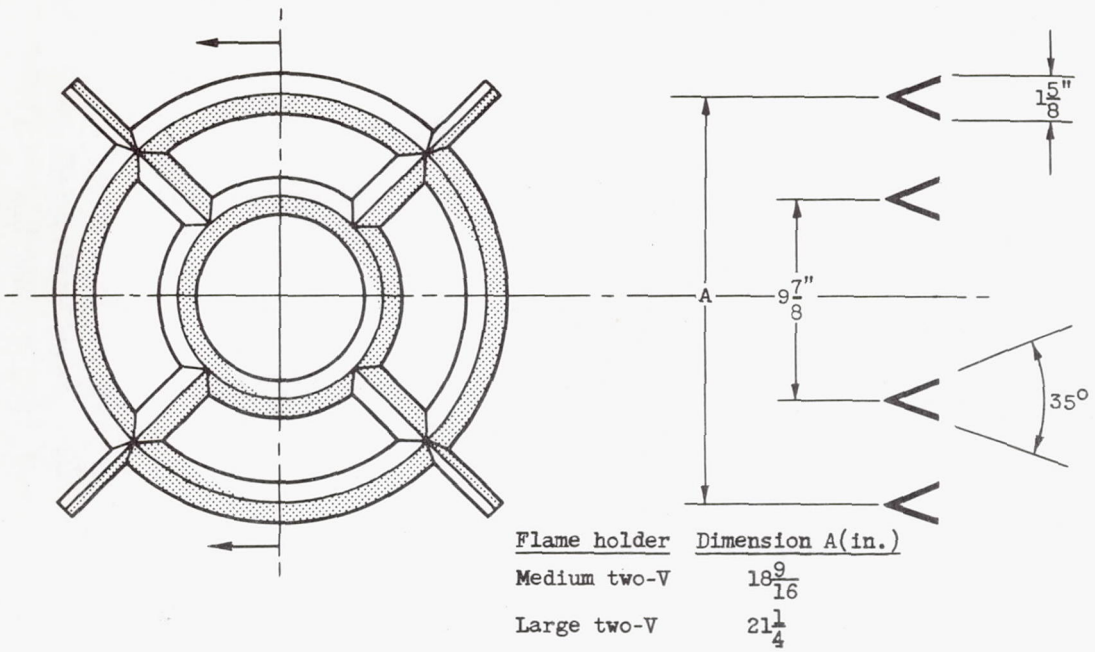

Flame holder	Dimension A(in.)
Medium two-V	$18\frac{9}{16}$
Large two-V	$21\frac{1}{4}$

(a) Two-V flame holders.

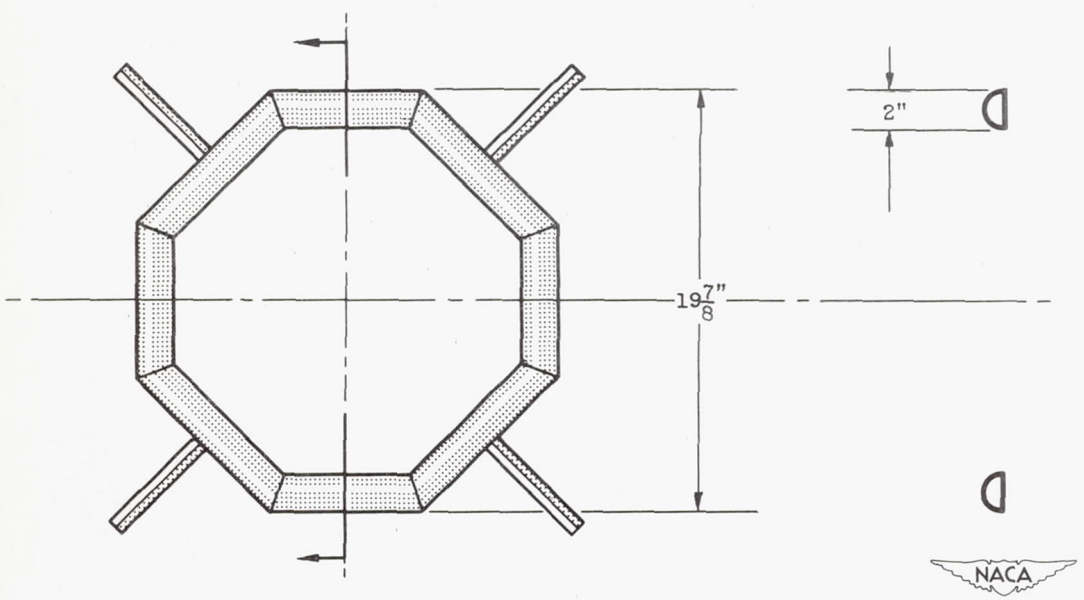

(b) Octagonal flame holder.

Figure 5. - Schematic diagram of flame holders.

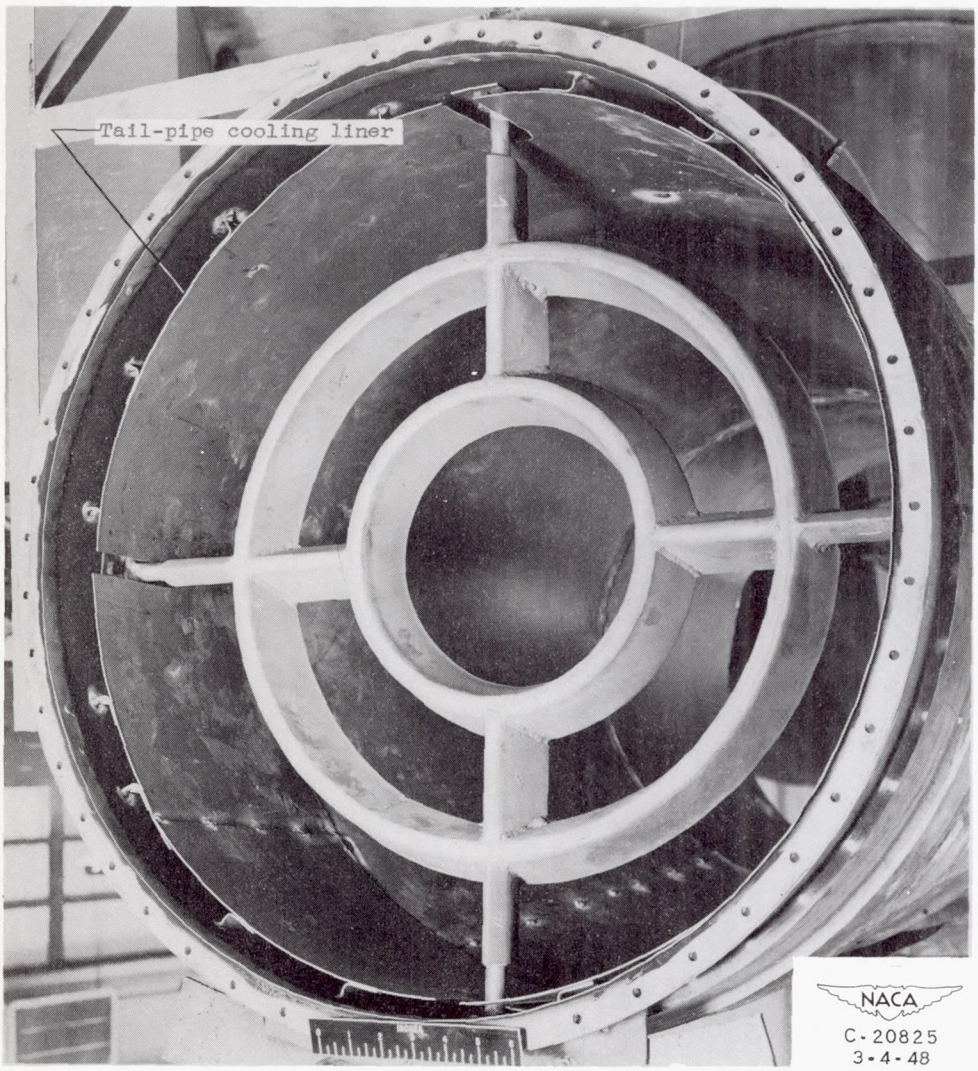

(a) Medium two-V flame-holder installation in configuration C; looking downstream.

Figure 6. - Photographs of flame holders.

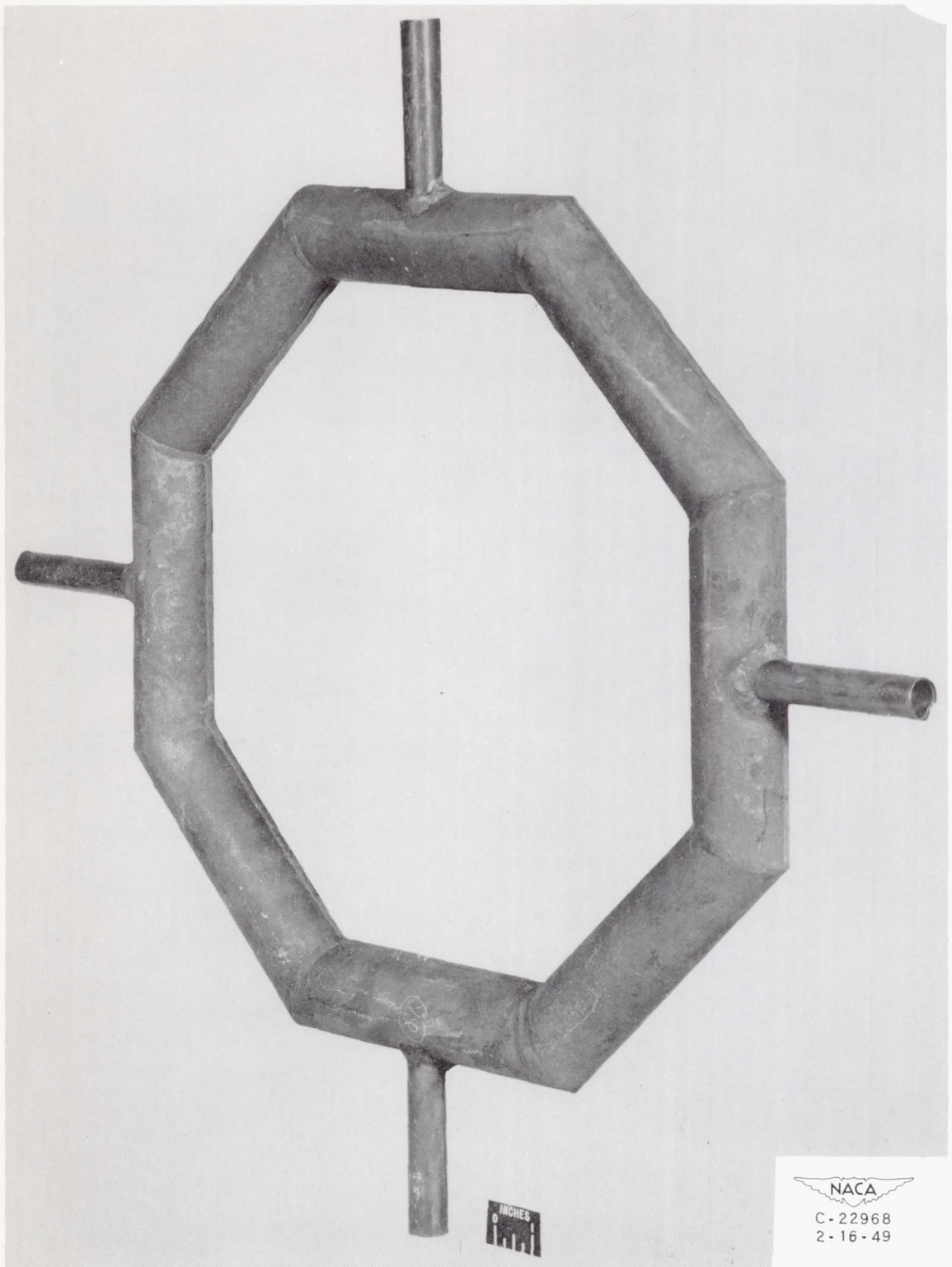

(b) Octagonal flame holder.

Figure 6. - Concluded. Photographs of flame holders.

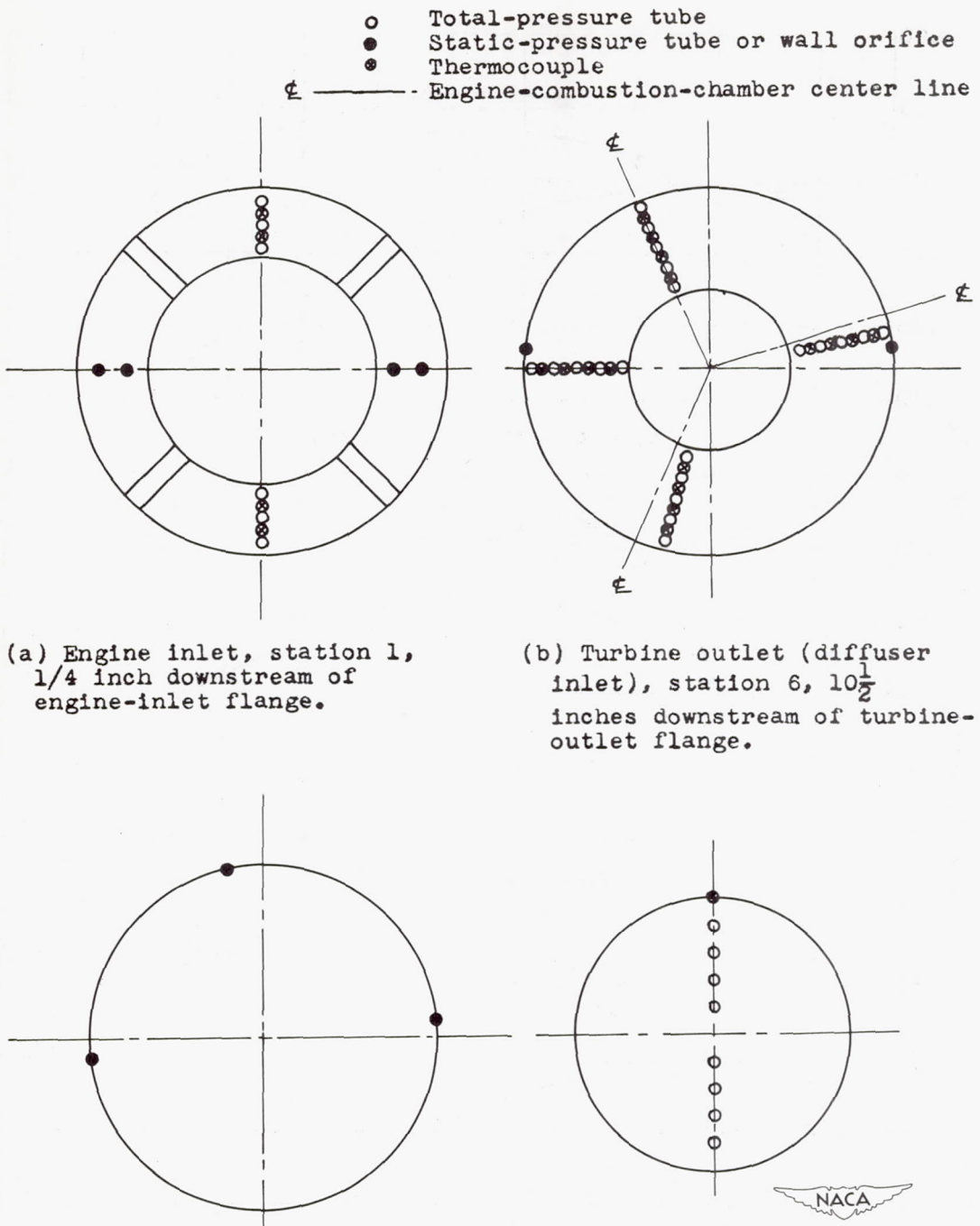

(a) Engine inlet, station 1, 1/4 inch downstream of engine-inlet flange.

(b) Turbine outlet (diffuser inlet), station 6, $10\frac{1}{2}$ inches downstream of turbine-outlet flange.

(c) Burner-section inlet, station 7, $8\frac{3}{4}$ inches upstream of flame holder.

(d) Exhaust nozzle, station 8, 1 inch upstream of outlet.

Figure 7. - Location of temperature and pressure instrumentation installed in engine and tail-pipe burner; looking downstream.

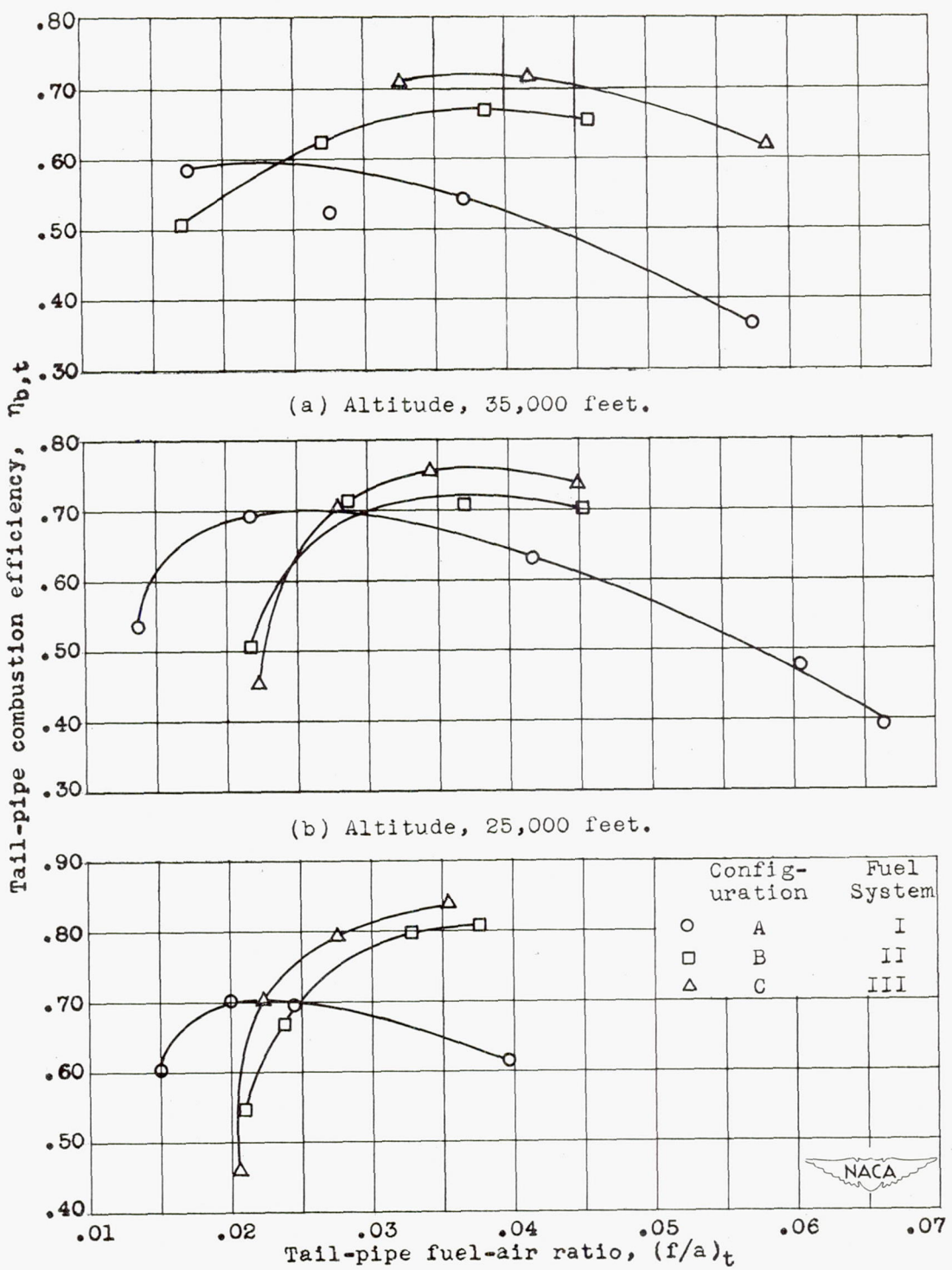

Figure 8. - Effect of tail-pipe fuel distribution on relation between tail-pipe combustion efficiency and tail-pipe fuel-air ratio. Medium two-V flame holder; simulated flight Mach number, 0.27.

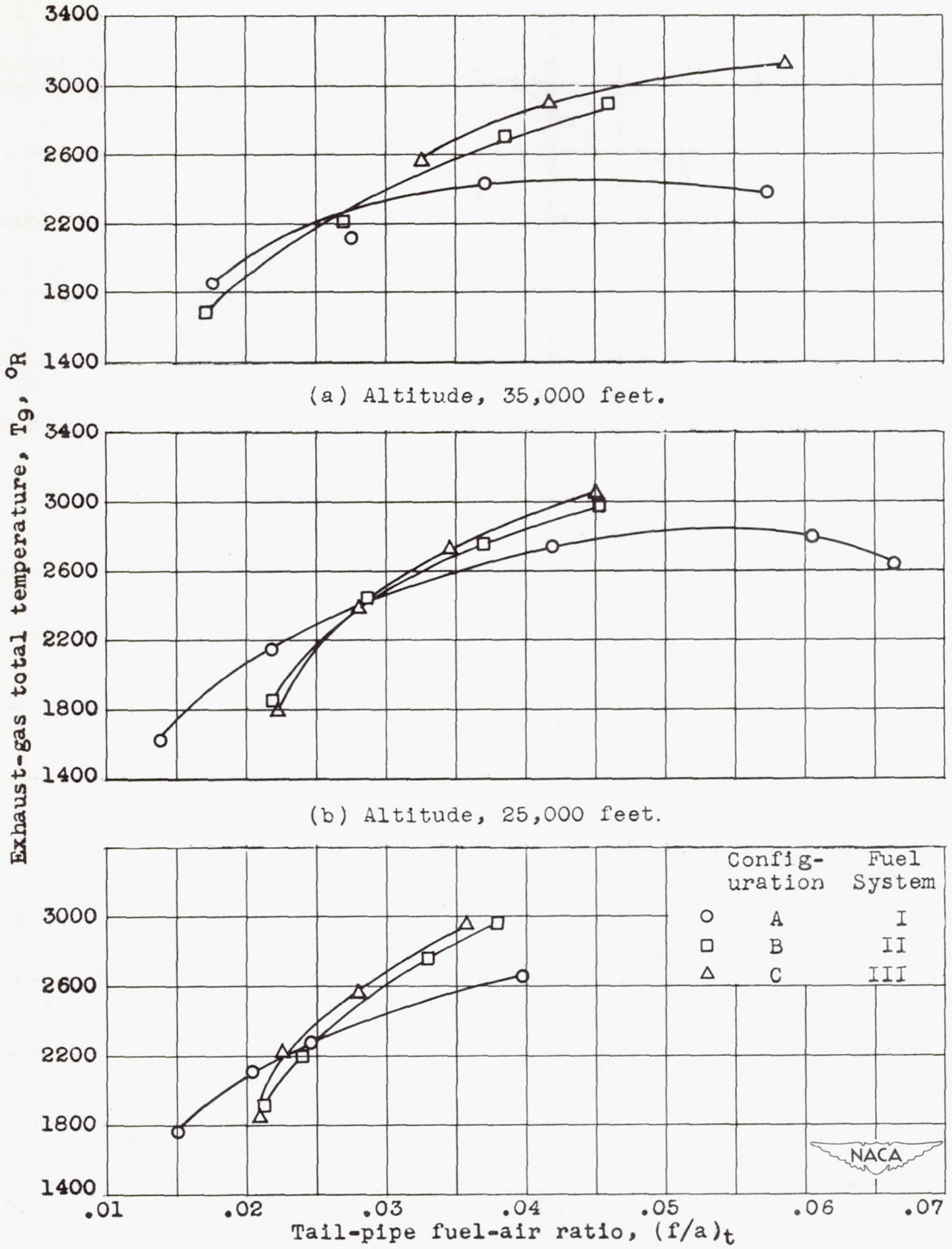

Figure 9. - Effect of tail-pipe fuel distribution on relation between exhaust-gas total temperature and tail-pipe fuel-air ratio. Medium two-V flame holder; simulated flight Mach number, 0.27.

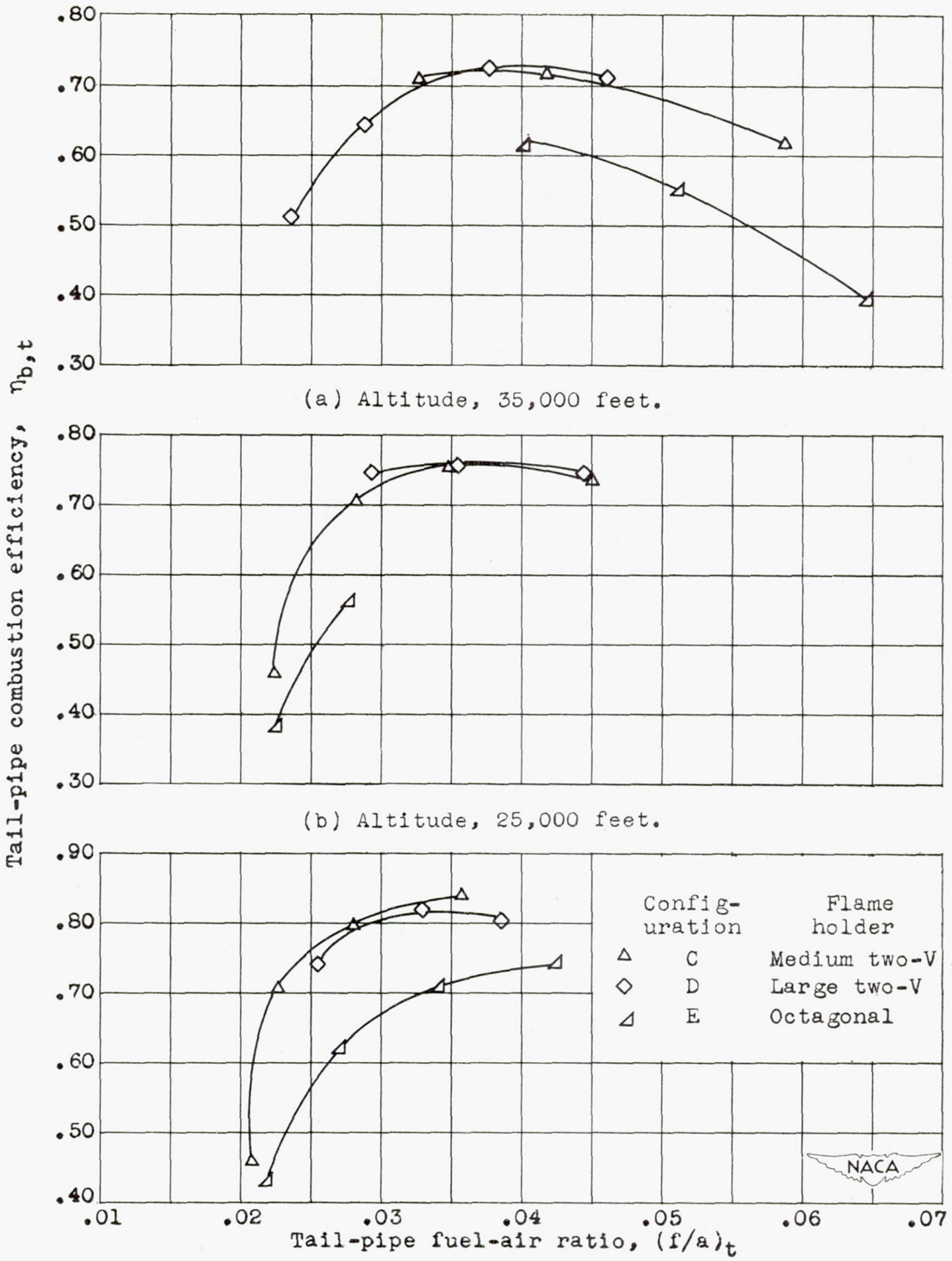

Figure 10. - Effect of flame-holder design on relation between tail-pipe combustion efficiency and tail-pipe fuel-air ratio. Fuel system III; simulated flight Mach number, 0.27.

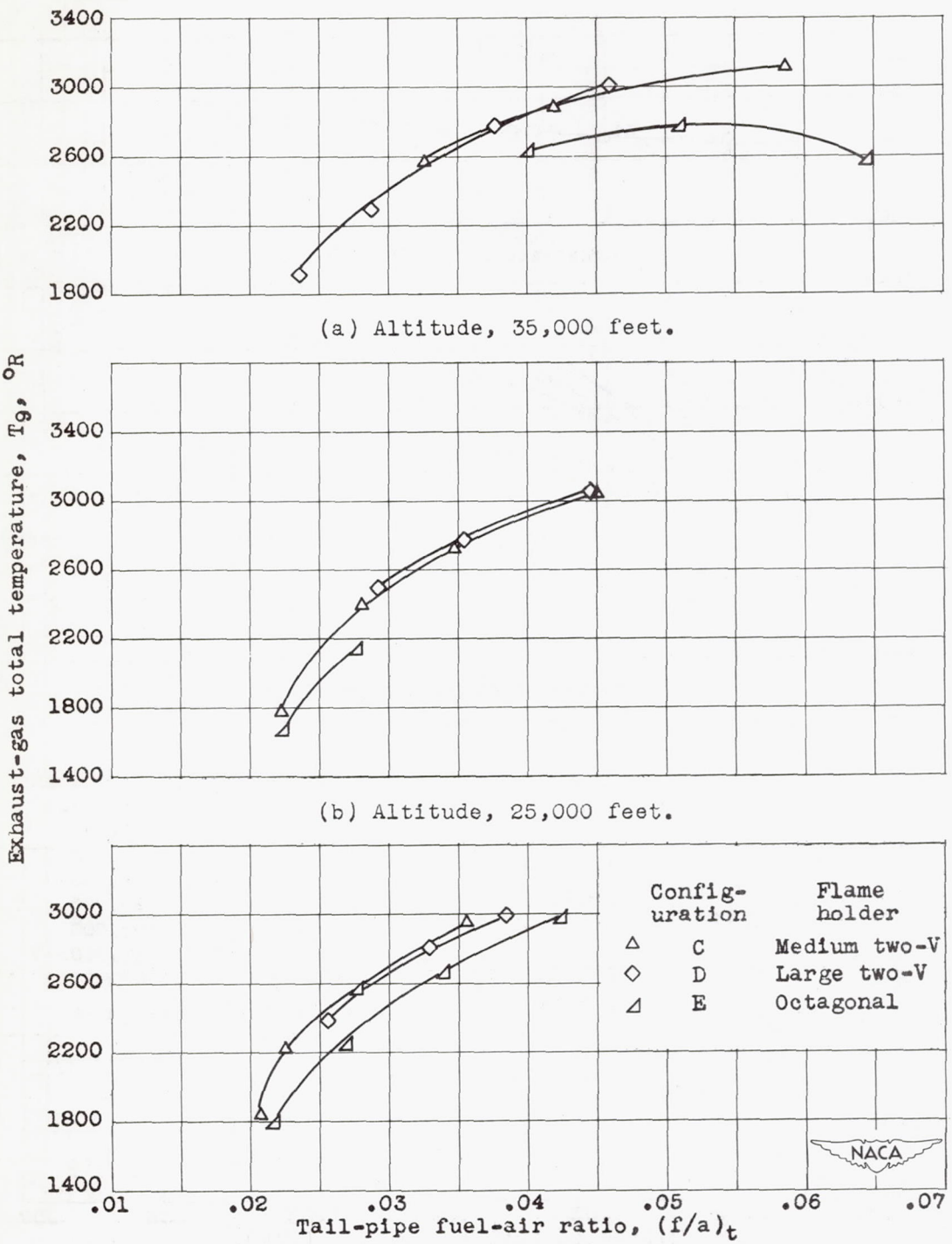

Figure 11. - Effect of flame-holder design on relation between exhaust-gas total temperature and tail-pipe fuel-air ratio. Fuel system III; simulated flight Mach number, 0.27.

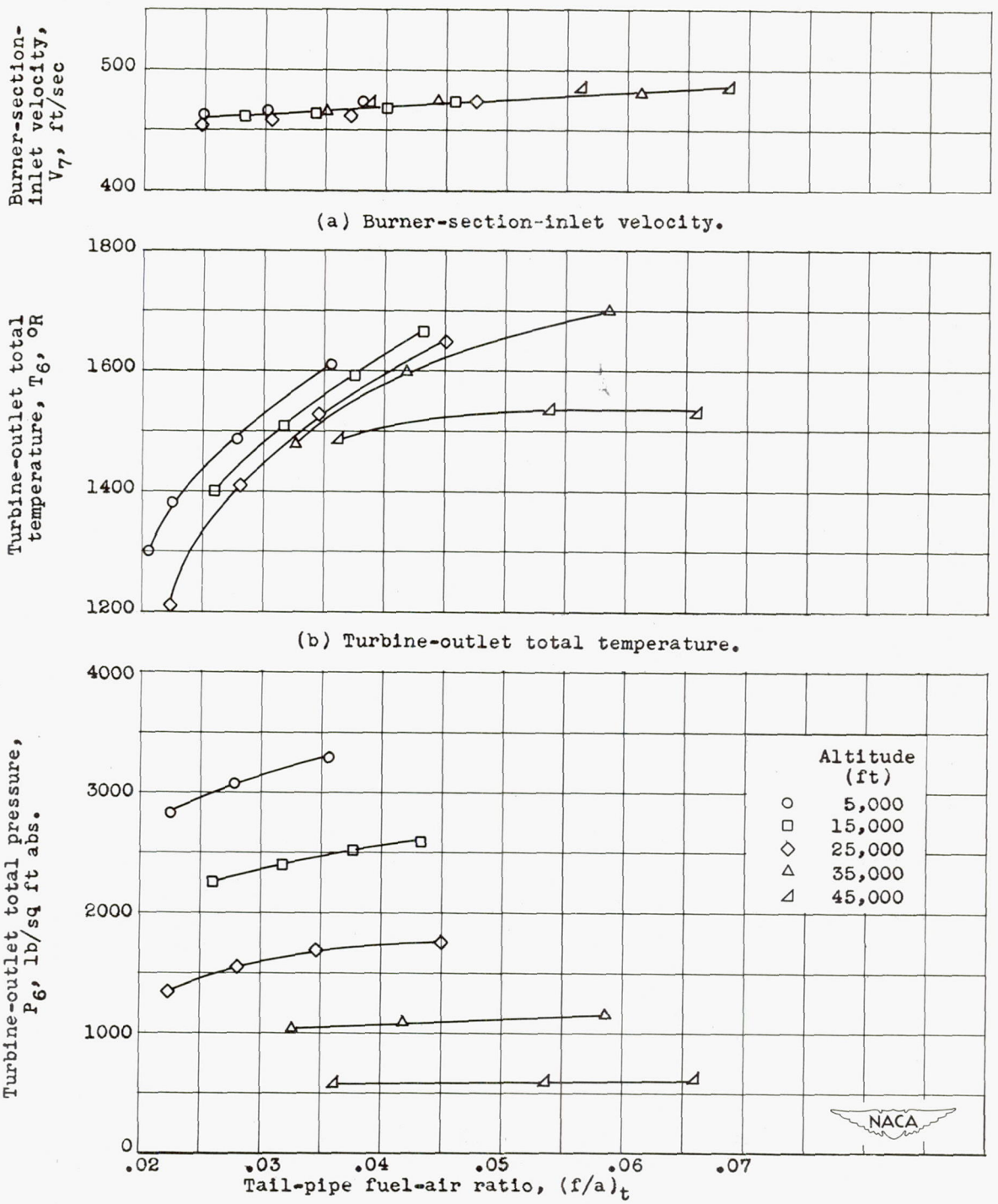

Figure 12. - Effect of altitude on tail-pipe burner-inlet conditions in configuration C. Simulated flight Mach number, 0.27.

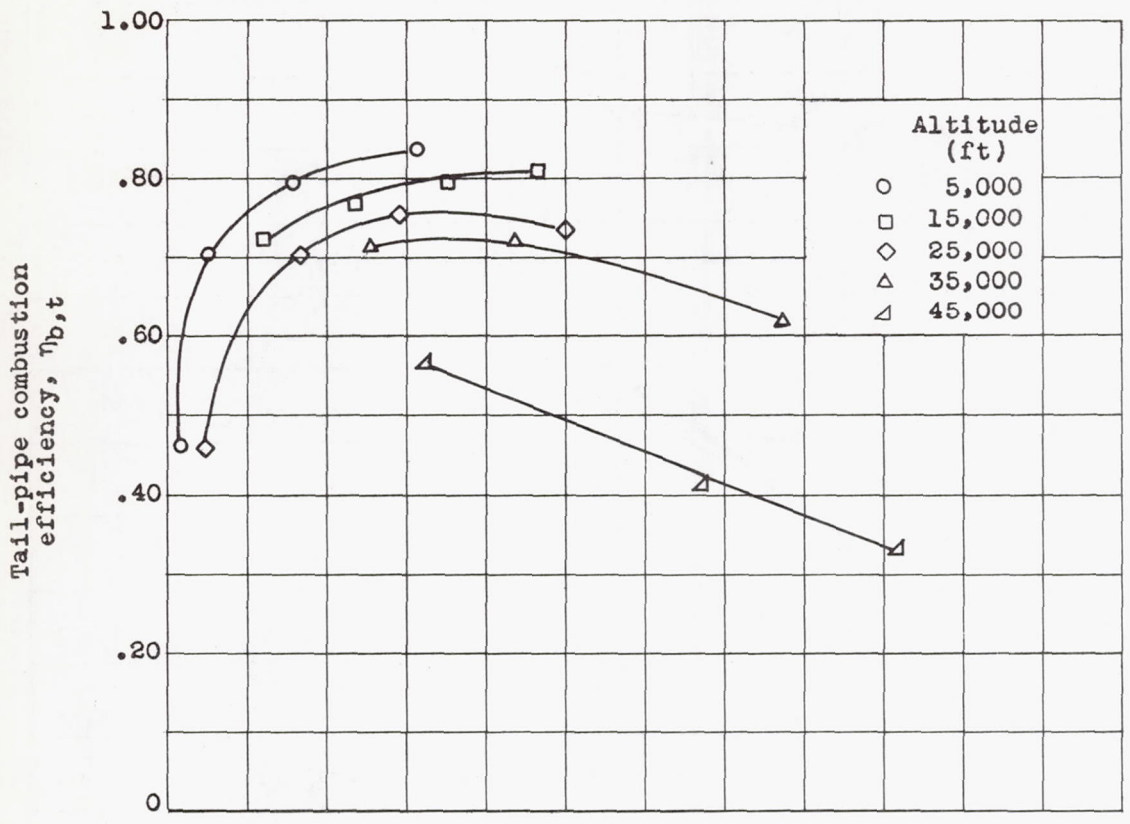

(a) Tail-pipe combustion efficiency.

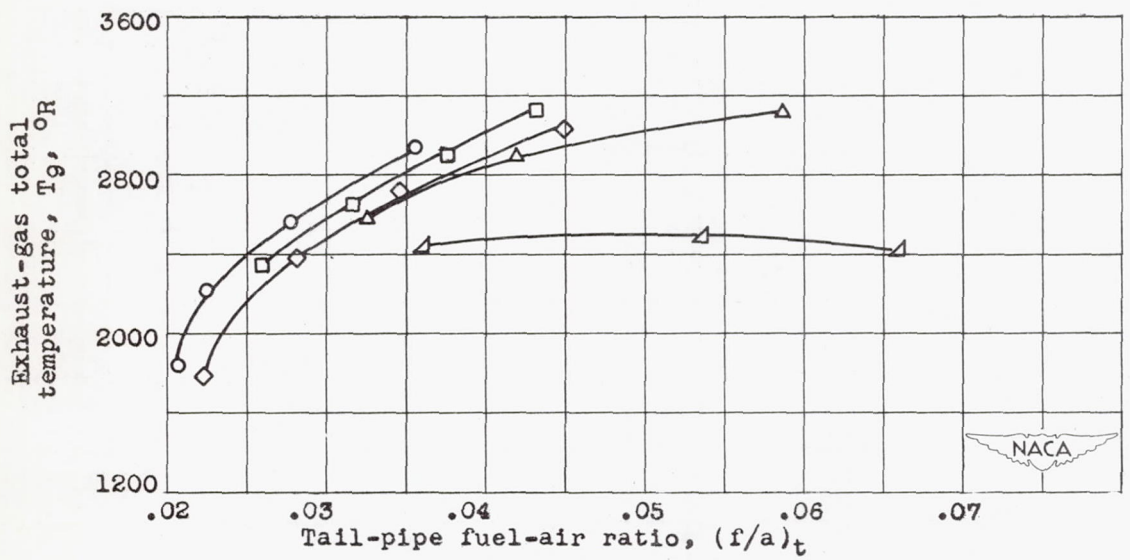

(b) Exhaust-gas total temperature.

Figure 13. - Effect of altitude on tail-pipe-burner performance of configuration C. Simulated flight Mach number, 0.27.

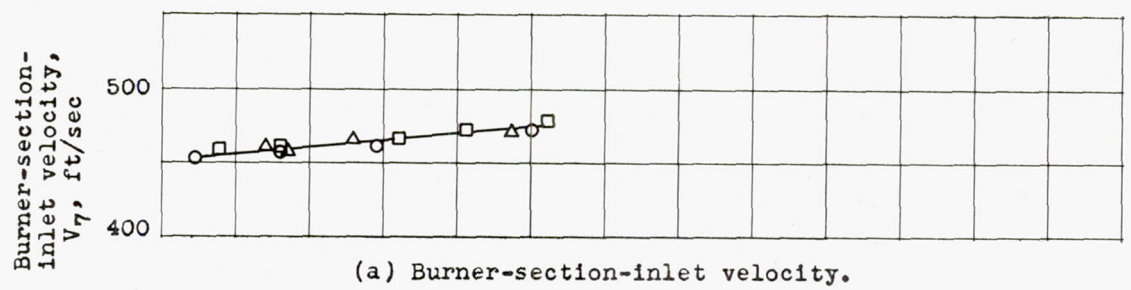

(a) Burner-section-inlet velocity.

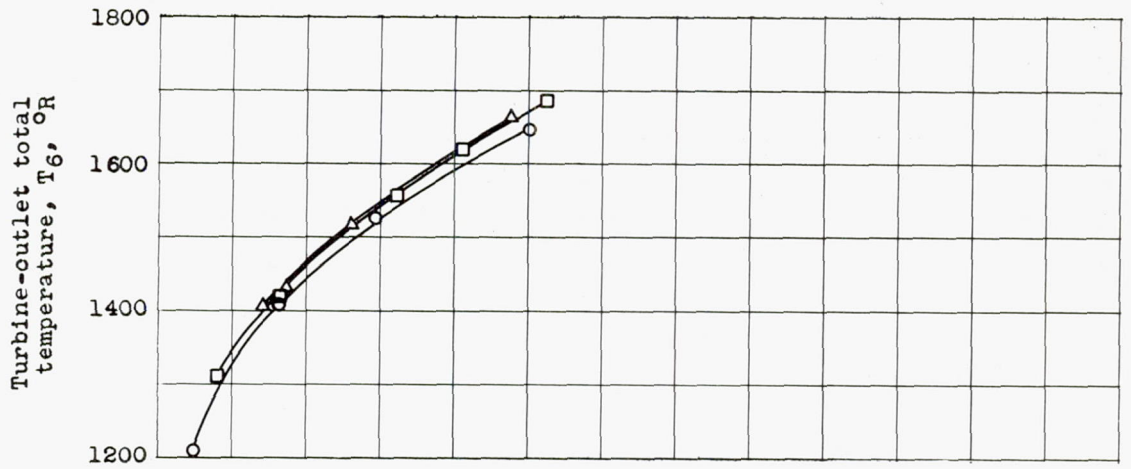

(b) Turbine-outlet total temperature.

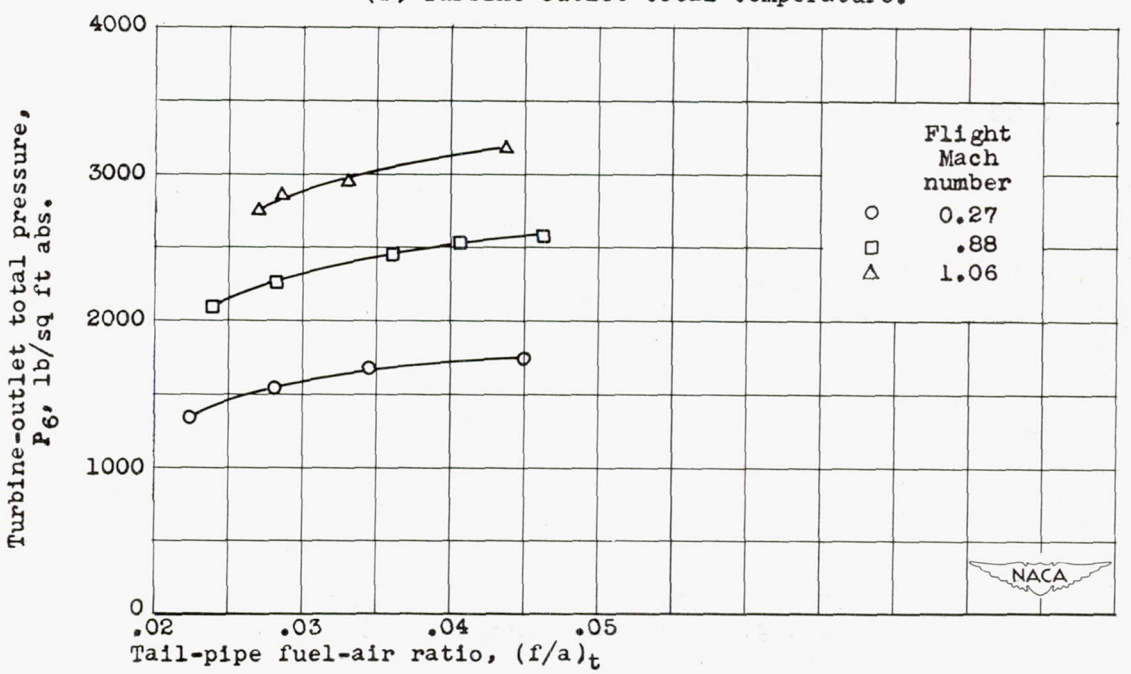

(c) Turbine-outlet total pressure.

Figure 14. - Effect of flight Mach number on tail-pipe burner-inlet conditions in configuration C. Altitude, 25,000 feet.

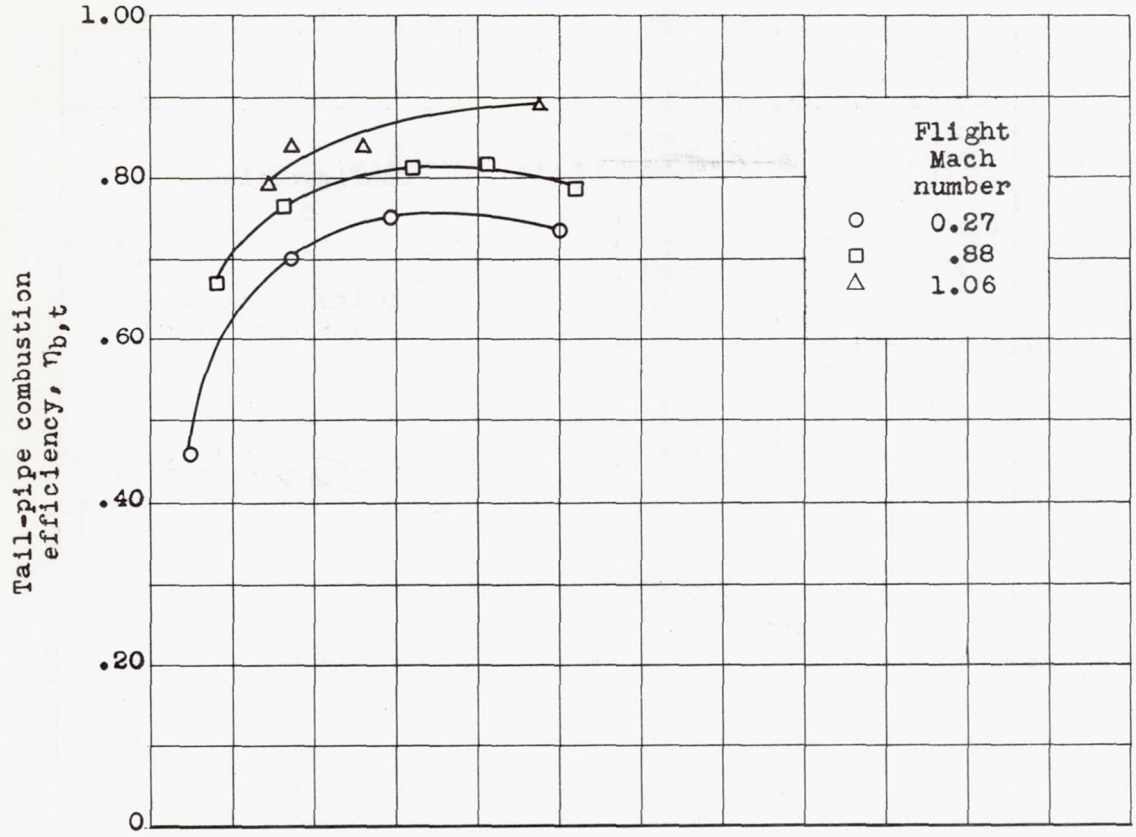

(a) Tail-pipe combustion efficiency.

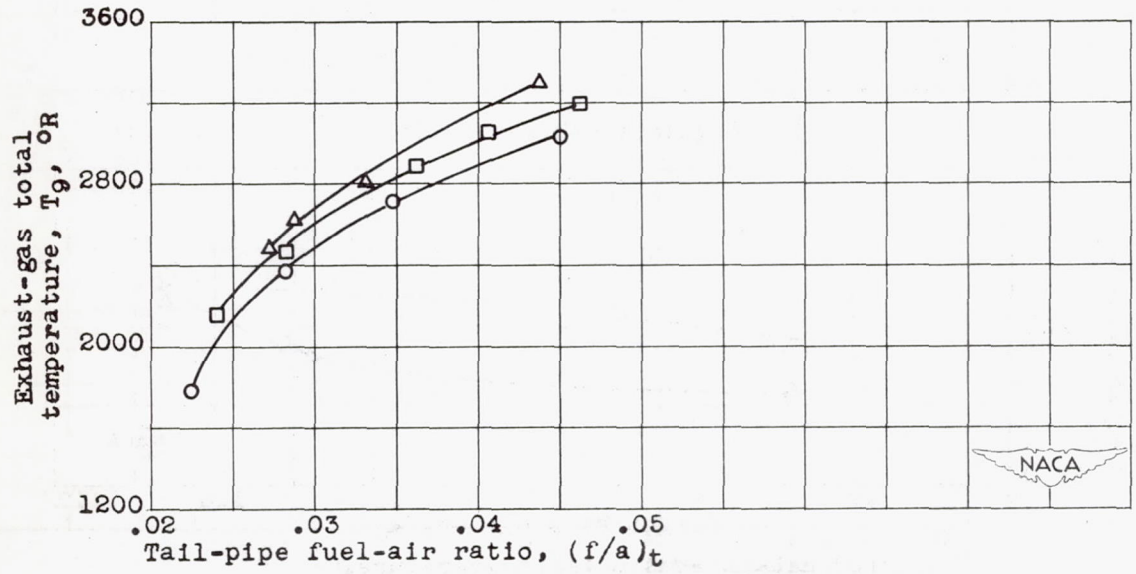

(b) Exhaust-gas total temperature.

Figure 15. - Effect of flight Mach number on tail-pipe-burner performance of configuration C. Altitude, 25,000 feet.

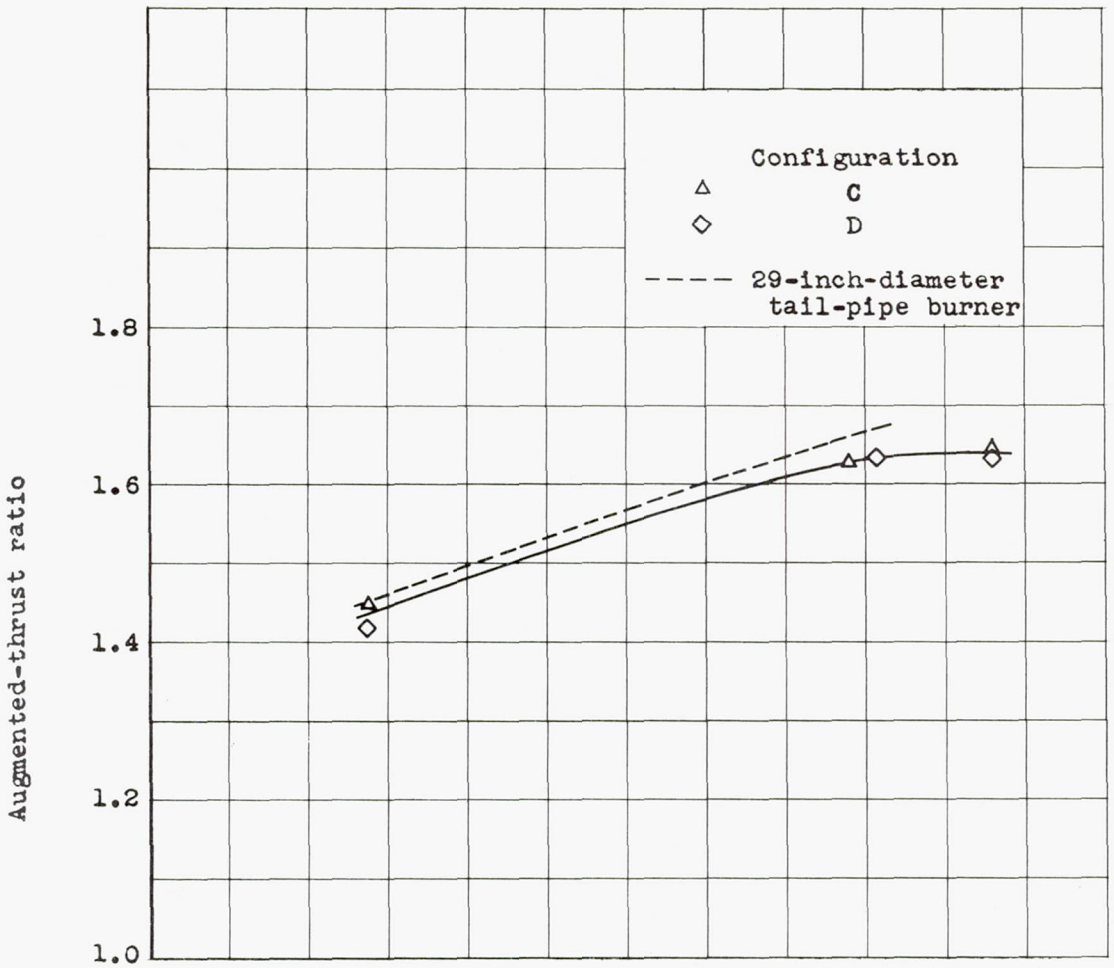

(a) Augmented-thrust ratio.

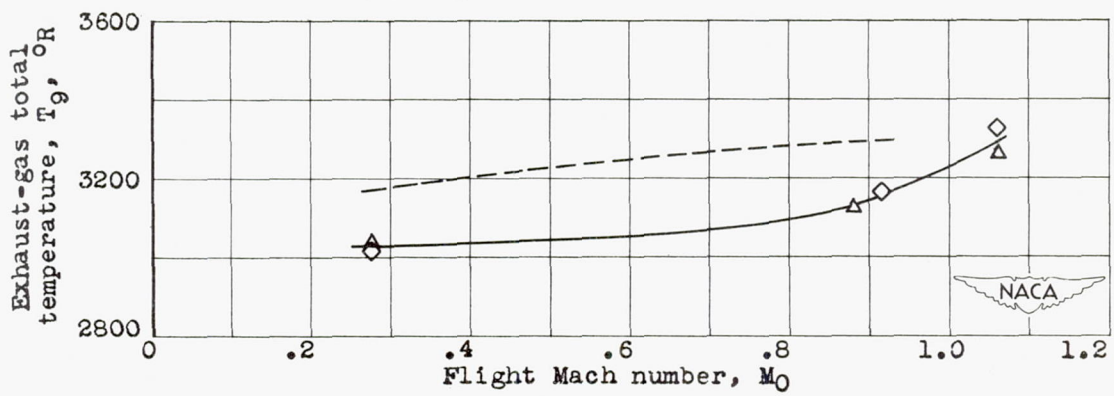

(b) Exhaust-gas total temperature.

Figure 16. - Relation between over-all performance characteristics and flight Mach number. Turbine-outlet total temperature, 1650° R; altitude, 25,000 feet; exhaust-nozzle-outlet area, 296 square inches. (Data for 29-inch-diameter tail-pipe burner obtained from reference 5.)

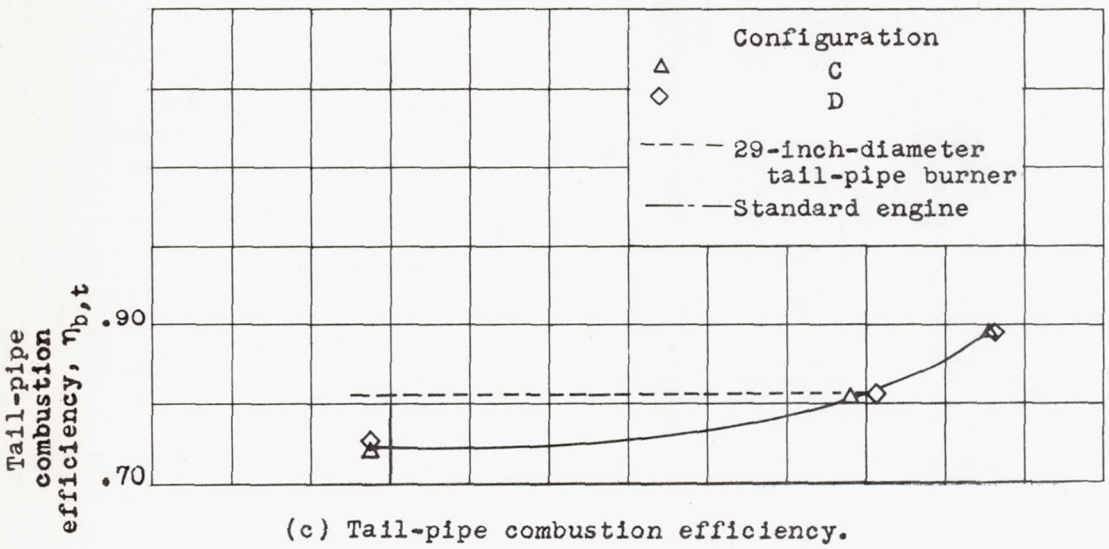

(c) Tail-pipe combustion efficiency.

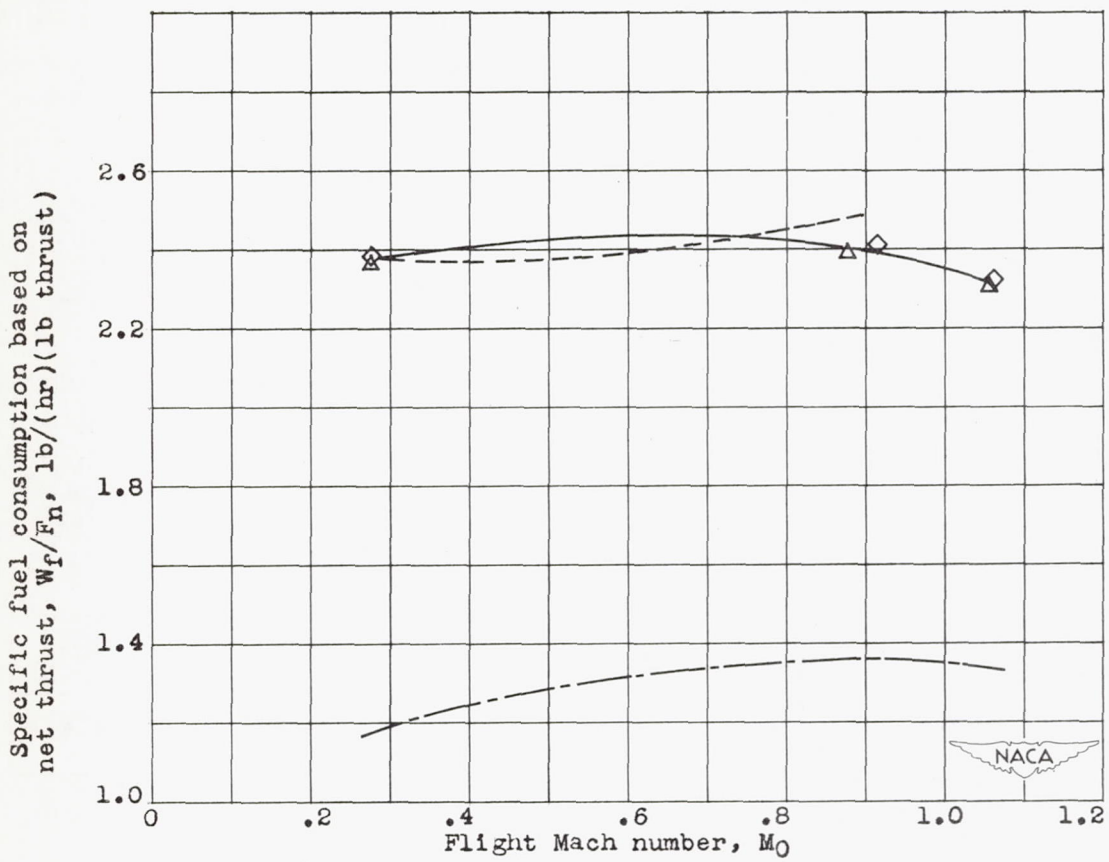

(d) Specific fuel consumption.

Figure 16. - Concluded. Relation between over-all performance characteristics and flight Mach number. Turbine-outlet total temperature, 1650° R; altitude, 25,000 feet; exhaust-nozzle-outlet area, 296 square inches. (Data for 29-inch-diameter tail-pipe burner obtained from reference 5.)

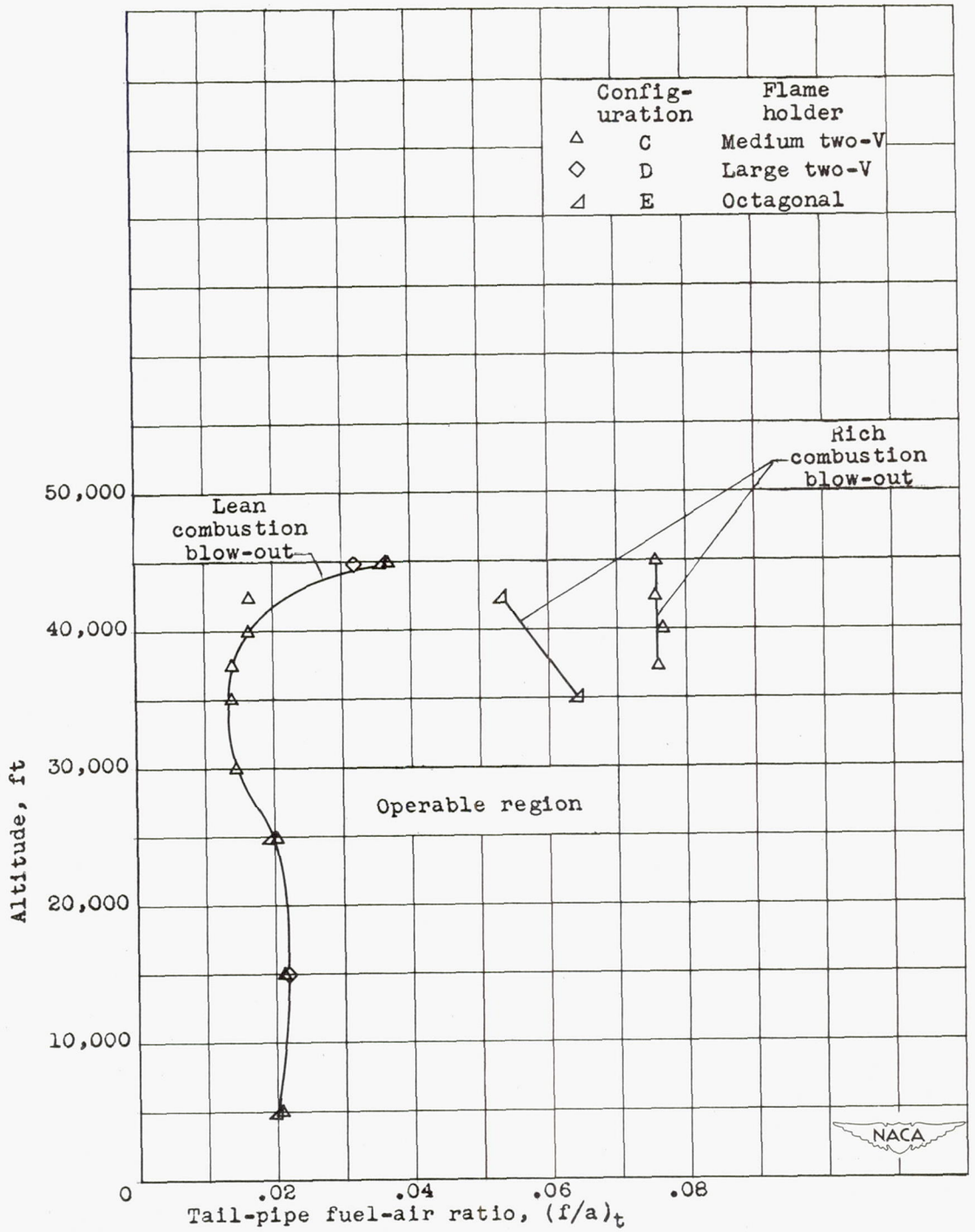

Figure 17. - Effect of flame-holder design on tail-pipe-burner combustion limits. Fuel system III; simulated flight Mach number, 0.27; exhaust-nozzle-outlet area, 296 square inches.